for hepatitis C virus genotype 4a and evidence for cross-genotype neutralization. Proc. Natl. Acad. Sci. U. S. A. **105**:997–1002.
26. **Shavinskaya A, Boulant S, Penin F, McLauchlan J, Bartenschlager R.** 2007. The lipid droplet binding domain of hepatitis C virus core protein is a major determinant for efficient virus assembly. J. Biol. Chem. **282**: 37158–37169.
27. **Suda G, et al.** 2010. IL-6-mediated intersubgenotypic variation of interferon sensitivity in hepatitis C virus genotype 2a/2b chimeric clones. Virology **407**:80–90.
28. **Takeuchi T, et al.** 1999. Real-time detection system for quantification of hepatitis C virus genome. Gastroenterology **116**:636–642.
29. **Wakita T, et al.** 2005. Production of infectious hepatitis C virus in tissue culture from a cloned viral genome. Nat. Med. **11**:791–796.
30. **Yi M, Ma Y, Yates J, Lemon SM.** 2007. Compensatory mutations in E1, p7, NS2, and NS3 enhance yields of cell culture-infectious intergenotypic chimeric hepatitis C virus. J. Virol. **81**:629–638.
31. **Yi M, Villanueva RA, Thomas DL, Wakita T, Lemon SM.** 2006. Production of infectious genotype 1a hepatitis C virus (Hutchinson strain) in cultured human hepatoma cells. Proc. Natl. Acad. Sci. U. S. A. **103**:2310–2315.
32. **Zhong J, et al.** 2005. Robust hepatitis C virus infection in vitro. Proc. Natl. Acad. Sci. U. S. A. **102**:9294–9299.

Biomaterials 33 (2012) 4526–4534

Contents lists available at SciVerse ScienceDirect

Biomaterials

journal homepage: www.elsevier.com/locate/biomaterials

The promotion of hepatic maturation of human pluripotent stem cells in 3D co-culture using type I collagen and Swiss 3T3 cell sheets

Yasuhito Nagamoto [a,b], Katsuhisa Tashiro [b], Kazuo Takayama [a,b], Kazuo Ohashi [d], Kenji Kawabata [b,c], Fuminori Sakurai [a], Masashi Tachibana [a], Takao Hayakawa [e,f], Miho Kusuda Furue [g,h], Hiroyuki Mizuguchi [a,b,i,*]

[a] Laboratory of Biochemistry and Molecular Biology, Graduate School of Pharmaceutical Sciences, Osaka University, Osaka 565-0871, Japan
[b] Laboratory of Stem Cell Regulation, National Institute of Biomedical Innovation, Osaka 567-0085, Japan
[c] Laboratory of Biomedical Innovation, Graduate School of Pharmaceutical Sciences, Osaka University, Osaka 565-0871, Japan
[d] Institute of Advanced Biomedical Engineering and Science, Tokyo Women's Medical University, Tokyo 162-8666, Japan
[e] Pharmaceutics and Medical Devices Agency, Tokyo 100-0013, Japan
[f] Pharmaceutical Research and Technology Institute, Kinki University, Osaka 577-8502, Japan
[g] Laboratory of Cell Cultures, Department of Disease Bioresources, National Institute of Biomedical Innovation, Osaka 567-0085, Japan
[h] Laboratory of Cell Processing, Institute for Frontier Medical Sciences, Kyoto University, Kyoto 606-8507, Japan
[i] The Center for Advanced Medical Engineering and Informatics, Osaka University, Osaka 565-0871, Japan

ARTICLE INFO

Article history:
Received 16 February 2012
Accepted 3 March 2012
Available online 23 March 2012

Keywords:
Hepatocyte
Co-culture
Collagen
Fibroblast
Liver
ECM (extracellular matrix)

ABSTRACT

Hepatocyte-like cells differentiated from human embryonic stem cells (hESCs) or human induced pluripotent stem cells (hiPSCs) are known to be a useful cell source for drug screening. We recently developed an efficient hepatic differentiation method from hESCs and hiPSCs by sequential transduction of FOXA2 and HNF1α. It is known that the combination of three-dimensional (3D) culture and co-culture, namely 3D co-culture, can maintain the functions of primary hepatocytes. However, hepatic maturation of hESC- or hiPSC-derived hepatocyte-like cells (hEHs or hiPHs, respectively) by 3D co-culture systems has not been examined. Therefore, we utilized a cell sheet engineering technology to promote hepatic maturation. The gene expression levels of hepatocyte-related markers (such as cytochrome P450 enzymes and conjugating enzymes) and the amount of albumin secretion in the hEHs or hiPHs, which were 3D co-cultured with the Swiss 3T3 cell sheet, were significantly up-regulated in comparison with those in the hEHs or hiPHs cultured in a monolayer. Furthermore, we found that type I collagen synthesized in Swiss 3T3 cells plays an important role in hepatic maturation. The hEHs or hiPHs that were 3D co-cultured with the Swiss 3T3 cell sheet would be powerful tools for medical applications, such as drug screening.

1. Introduction

Several studies have recently shown the ability of human embryonic stem cells (hESCs) [1] and human induced pluripotent stem cells (hiPSCs) [2] to differentiate into hepatocyte-like cells [3–6]. Although primary human hepatocytes are generally employed for drug toxicity screening in the early phase of pharmaceutical development, these cells have some drawbacks, such as their limited range of sources, difference in variability and functions from batch to batch, and de-differentiation. Because hESC- or hiPSC-derived hepatocyte-like cells (hEHs or hiPHs, respectively) have potential to resolve these problems, they are expected to be applied to drug screening. The hepatic differentiation processes from hESCs and hiPSCs are divided into three-stages, differentiation into definitive endoderm (DE) cells, hepatoblasts, and mature hepatocytes. Hepatic differentiation methods based on the treatment of growth factors have been widely used to generate hepatocyte-like cells from hESCs or hiPSCs [5–9]. However, the hepatic differentiation efficiency is not high enough for medical applications such as drug screening [10]. To promote the efficiency of hepatic differentiation and hepatic maturation, we have developed hepatic differentiation methods that combine the transduction of transcription factor genes involved in liver development

* Corresponding author. Laboratory of Biochemistry and Molecular Biology, Graduate School of Pharmaceutical Sciences, Osaka University, 1-6 Yamadaoka, Suita, Osaka 565-0871, Japan. Tel.: +81 6 6879 8185; fax: +81 6 6879 8186.
E-mail address: mizuguch@phs.osaka-u.ac.jp (H. Mizuguchi).

0142-9612/$ – see front matter © 2012 Elsevier Ltd. All rights reserved.
doi:10.1016/j.biomaterials.2012.03.011

with stimulation by growth factors [11–13]. The hepatocyte-like cells generated by our protocols have levels of expression of hepatocyte-related genes similar to the levels in (cryopreserved) primary human hepatocytes cultured for 48 h after plating [12]. Moreover, we have recently established more efficient and simple methods for hepatic differentiation from hESCs and hiPSCs by sequential transduction of forkhead box A2 (FOXA2) and hepatocyte nuclear factor 1 homeobox A (HNF1α) (in submitted). In that recent study, we showed that the hEHs or hiPHs expressed the genes of hepatocyte-related markers at levels similar to those in primary human hepatocytes and could metabolize various types of drugs.

It is known that cell–cell interactions between hepatocytes and their surrounding cells are essential for liver development and maintenance of liver functions [14–17]. Although primary human hepatocytes rapidly lose their functions under a monolayer culture condition, they could retain their functions, such as albumin secretion and urea synthesis, in three-dimensional (3D) culture and co-culture [18–21]. Moreover, it has been reported that the primary hepatocytes maintain their functions for a long time by the combination of 3D culture and co-culture, namely 3D co-culture [22–24]. In particular, the functions of primary rat hepatocytes cultured in a 3D co-culture, were shown to be more efficiently preserved than the functions of primary rat hepatocytes cultured in monolayer a co-culture [24]. Recently, Kim et al. reported that primary rat hepatocytes are able to maintain their functions in 3D co-culture with an endothelial cell sheet [25]. To perform 3D co-culture with a cell sheet, they employed cell sheet engineering technology using temperature-responsive culture dishes grafted with a temperature-responsive polymer, poly(*N*-isopropylacrylamide). This cell sheet engineering technology make it possible to manipulate a monolayer cell sheet with the extracellular matrices (ECMs) synthesized from the cells [26]. Although 3D culture or co-culture methods have been individually applied to promote hepatic differentiation from ESCs or iPSCs [27–29], few studies have investigated the hepatic differentiation from hESCS or hiPSCs using a 3D co-culture method.

In this study, we examined whether 3D co-culture, which uses the cell sheet engineering technology, could promote hepatic differentiation, and particularly the differentiation into mature hepatocyte-like cells, from hESCs and hiPSCs. Because Swiss 3T3 cells are widely used for co-culture with primary hepatocytes [18–20], we employed Swiss 3T3 cells for 3D co-culture with the hEHs or hiPHs. After hEHs and hiPHs were 3D co-cultured with a Swiss 3T3 cell sheet, we examined the expression levels of hepatocyte-related genes. Moreover, we investigated a Swiss 3T3 cell-derived factor that can promote hepatic maturation from hESCs and hiPSCs.

2. Materials and methods

2.1. hESC and hiPSC culture

A hESC line, H9 (WiCell Research Institute), was maintained on a feeder layer of mitomycin C (MMC)-treated mouse embryonic fibroblasts (MEF, Millipore) with ReproStem (ReproCELL) supplemented with 5 ng/ml fibroblast growth factor 2 (FGF2) (Sigma). hESCs were dissociated with 0.1 mg/ml dispase (Roche Diagnostics) into small clumps and were then subcultured every 4 or 5 days. H9 cells were was used following the Guidelines for Derivation and Utilization of Human Embryonic Stem Cells of the Ministry of Education, Culture, Sports, Science and Technology of Japan. One hiPSC line generated from the human embryonic lung fibroblast cell line MCR5 was provided from the JCRB Cell Bank (Tic, JCRB Number: JCRB1331). Another hiPSC line, 201B7, generated from human dermal fibroblasts was kindly provided by Dr. S. Yamanaka (KyotoUniversity). These hiPSC lines were maintained on a feeder layer of MMC-treated MEF with iPSellon (for Tic, Cardio) or ReproStem (for 201B7, ReproCELL) supplemented with 10 ng/ml (for Tic) or 5 ng/ml (for 201B7) FGF2.hiPSCs were dissociated with 0.1 mg/ml dispase (Roche Diagnostics) into small clumps and were then subcultured every 5 or 6 days.

2.2. Swiss 3T3 cell culture

A mouse fibroblast line, Swiss 3T3, was maintained with RPMI-1640 medium (Sigma) supplemented with fetal bovine serum (10%) (FBS), streptomycin (120 μg/ml), and penicillin (200 μg/ml).

2.3. Ad vectors

The human eukaryotic translation elongation factor 1 alpha 1 (EF-1α) promoter-driven HNF1α- and FOXA2-expressing Ad vectors (Ad-HNF1α and Ad-FOXA2, respectively) were constructed previously (in submitted). All of Ad vectors contain a stretch of lysine residue (K7) peptides in the C-terminal region of the fiber knob for more efficient transduction of hESCs, hiPSCs, and DE cells, in which transduction efficiency was almost 100%, and purified as described previously [11,12,30]. The vector particle (VP) titer was determined by using a spectrophotometric method [31].

2.4. In vitro differentiation

Before the initiation of cellular differentiation, the medium of hESCs and hiPSCs was exchanged for a defined serum-free medium, hESF9, and hESCs and hiPSCs were cultured as previously reported [32]. The differentiation protocol for the induction of DE cells, hepatoblasts, and hepatocytes was based on our previous report with some modifications (in submitted). Briefly, in mesendoderm differentiation, hESCs and hiPSCs were dissociated into single cells by using Accutase (Millipore) and cultured for 2 days on Matrigel (BD Biosciences) in hESF-DIF medium (Cell Science & Technology Institute) supplemented with 10 μg/ml human recombinant insulin, 5 μg/ml human apotransferrin, 10 μM 2-mercaptoethanol, 10 μM ethanolamine, 10 μM sodium selenite, and 0.5 mg/ml bovine serum albumin (BSA) (all from Sigma) (differentiation hESF-DIF medium) containing 100 ng/ml Activin A (R&D Systems) and 10 ng/ml FGF2. To generate DE cells, hESC- or hiPSC-derived mesendoderm cells were transduced with 3000 VP/cell of Ad-FOXA2 for 1.5 h on day 2 and cultured until day 6 on Matrigel in differentiation hESF-DIF medium supplemented with 100 ng/ml Activin A and 10 ng/ml FGF2. For induction of the hepatoblasts, the hESC- or hiPSC-derived DE cells were transduced with each 1500 VP/cell of Ad-FOXA2 and Ad-HNF1α for 1.5 h on day 6 and cultured for 3 days on Matrigel in hepatocyte culture medium (HCM) (Lonza) supplemented with 30 ng/ml bone morphogenetic protein 4 (BMP4) and 20 ng/ml FGF4 (all from R&D Systems). To expand the hepatoblasts, the hepatoblasts were transduced with each 1500 VP/cell of Ad-FOXA2 and Ad-HNF1α for 1.5 h on day 9 and cultured for 3 days on Matrigel in HCM supplemented with 10 ng/ml hepatocyte growth factor (HGF), 10 ng/ml FGF1, 10 ng/ml FGF4, and 10 ng/ml FGF10 (all from R&D Systems).To induce hepatic maturation, the cells were cultured for 2 days on Matrigel in L15 medium (Invitrogen) supplemented with 8.3% tryptose phosphate broth (BD Biosciences), 10% FBS (Vita), 10 μM hydrocortisone 21-hemisuccinate (Sigma), 1 μM insulin, and 25 mM NaHCO3 (Wako) (differentiation L15 medium) containing 20 ng/ml hepatocyte growth factor (HGF), 20 ng/ml Oncostatin M (OsM) (R&D Systems), and 10^{-6} M Dexamethasone (DEX) (Sigma). As described below, the Swiss 3T3 cell sheet was stratified onto hepatocyte-like cells on day 14 and cultured in differentiation L15 medium supplemented with 20 ng/ml HGF, 20 ng/ml OsM, and 10^{-6} M DEX until day 15. On day 15, Matrigel was stratified onto the cells and cultured in differentiation L15 medium supplemented with 20 ng/ml HGF, 20 ng/ml OsM, and 10^{-6} M DEX until day 25.

2.5. Cell sheet harvesting and stratifying procedure utilizing a gelatin-coated manipulator

The stratifying protocol was performed as previously described with some modifications [25,33]. Briefly, Swiss 3T3 cells were seeded on a 24-well temperature-responsive culture plate (TRCP) (Cell Seed Inc, Tokyo) on day 12. Two days after seeding (day 14), Swiss 3T3 cells were grown to confluence. On the same day (day 14), a gelatin-coated cell sheet manipulator was placed on the Swiss 3T3 cells, and the culture temperature was reduced to 20 °C for 60 min. By removing the manipulator, cultured Swiss 3T3 cells were harvested as a contiguous cell sheet that attached on the gelatin. The Swiss 3T3 cell sheet was then stratified on the hEHs or hiPHs. The culture plate with the manipulator was incubated at room temperature for 60 min to induce adherence between the hEHs or hiPHs and Swiss 3T3 cell sheet. To dissolve the gelatin, the culture plate was incubated at 37 °C for 60 min, and this was followed by several washing steps.

2.6. RNA isolation and reverse transcription-PCR

Total RNA was isolated from the hESC- or hiPSC-derived cells using ISOGENE (Nippon Gene) according to the manufacturer's instructions. cDNA was synthesized using 500 ng of total RNA with a Superscript VILO cDNA synthesis kit (Invitrogen). Real-time RT-PCR was performed with Taqman gene expression assays or Fast SYBR Green Master Mix using an ABI Step One Plus (all from Applied Biosystems). Relative quantification was performed against a standard curve and the values were normalized against the input determined for the housekeeping gene, *glyceraldehyde 3-phosphate dehydrogenase* (*GAPDH*). The primer sequences used in this study are described in Supplementary Tables 1 and 2.

2.7. Preparation of verticalsection

On day 15, the hEHs cultured with or without the Swiss 3T3 cell sheet were frozen in Tissue-Tek O.C.T. Compound (Sakura Finetek), then vertically sectioned and fixed with 4% paraformaldehyde. These sections were monitored by a phase contrast microscope (Olympus).

2.8. ELISA

hESCs or hiPSCs were differentiated into the hepatocyte-like cells as described in Fig. 1A. The culture supernatants, which were incubated for 24 h after fresh medium was added, were collected and analyzed to determine the amount of ALB secretion by ELISA. ELISA kits for ALB were purchased from Bethyl Laboratories. ELISA was performed according to the manufacturer's instructions. The amount of ALB secretion was calculated according to each standard.

2.9. Co-culture and culture in a cell culture insert system (insert-culture)

hESCs were differentiated into the hepatocyte-like cells as described in Fig. 1A until day 14, and then the hESC-derived cells were harvested and seeded onto a 6-well culture plate (Falcon) with Swiss 3T3 (1:1) in a co-culture system. In a insert-culture system, hESC-derived hepatocyte-like cells were harvested and seeded onto a 6-well culture plate alone, and Swiss 3T3 cells were plated in cell culture inserts (membrane pore size 1.0 μm; Falcon), and placed in a well of the culture palate containing hESC-derived hepatocyte-like cells. These cells were cultured in differentiation L15 medium supplemented with 20 ng/ml HGF, 20 ng/ml OsM, and 10^{-6} M DEX until day 25.

2.10. Stratification of type I collagen gel

A type I collagen gel solution was prepared as suggested by Nitta Gelatin: 7 parts of solubilized collagen in HC1 (pH 3.0) 2 parts of 5× concentrated RPMI-1640 medium, and 2 parts of reconstitution buffer (0.2 M HEPES, 0.08 M NaOH) to neutralize the collagen gel, were mixed gently but rapidly at 4 °C. Next, the hESC-derived cells were cultured in a type I collagen gel solution for 3h, and then the medium waschanged and the cells were cultured in differentiation L15 medium supplemented with 20 ng/ml HGF, 20 ng/ml OsM, and 10^{-6} M DEX until day 25.

2.11. Inhibition of collagen synthesis

hESCs were differentiated into the hepatocyte-like cells as described in Fig. 1A until stratification of the Swiss 3T3 cell sheet. After stratification of the Swiss 3T3 cell sheet, the cells were cultured in differentiation L15 medium supplemented with 20 ng/ml HGF, 20 ng/ml OsM, 10^{-6} M DEX, and 25 μM 2,2′-Bipyridyl (Wako), an inhibitor of collagen synthesis, until day 25.

2.12. Western blotting analysis

Swiss 3T3 cells were cultured with 25 μM 2,2′-Bipyridyl or solvent (0.1% DMSO) for 3 days, and these cells were then homogenized with lysis buffer (1% Nonidet P-40, 1 mM EDTA, 25 mM Tris-HCl, 5 mM NaF, and 150 mM NaCl) containing protease inhibitor mixture (Sigma-Aldrich). After being frozen and thawed, the homogenates were centrifuged at 15,000× *g* at 4 °C for 10 min, and the supernatants were collected. The lysates were subjected to SDS-PAGE on 7.5% polyacrylamide gel and were then transferred onto polyvinylidene fluoride membranes (Millipore). After the reaction was blocked with 1% skim milk in TBS containing 0.1% Tween 20 at room temperature for 1 h, the membranes were incubated with goat anti-col1a1 Ab (diluted 1/200; Santa Cruz Biotechnology) or mouse anti-β-actin Ab (diluted 1/5000; Sigma) at 4 °C overnight, followed by reaction with horseradish peroxidase-conjugated anti-goat IgG (Chemicon) or anti-mouse IgG (Cell Signaling Technology) at room temperature for 1 h. The band was visualized by ECL Plus Western blotting detection reagents (GE Healthcare) and the signals were read using a LAS-3000 imaging system (FUJI Film).

2.13. Statistical analysis

Statistical analysis was performed using the unpaired two-tailed Student's *t*-test.

3. Results

3.1. Efficient hepatic maturation by stratification of the Swiss 3T3 cell sheet

The hEHs, which were generated by the transduction of *HNF1α* and *FOXA2* genes, were 3D co-cultured with the Swiss 3T3 cell sheet to promote hepatic differentiation and to generate mature hepatocytes from hESCs and hiPSCs. Our differentiation strategy using the stratification of the Swiss 3T3 cell sheet is illustrated in Fig. 1A. The stratifying procedure was performed on day 14 as described in Fig. 1B. The day after stratifying the Swiss 3T3 cell sheet on the hEHs, vertical sections of the monolayer hEHs (hEHs-mono) and the hEHs stratified with the Swiss 3T3 cell sheet (hEHs-Swiss) were prepared (Fig. 1C). We found that Swiss 3T3 cells were successfully harvested and overlaid onto the hEHs as a monolayer cell sheet (Fig. 1C). Moreover, the hEHs seemed to be larger than the Swiss 3T3 cells. The space between the hEHs cells and Swiss 3T3 cells suggests the formation of ECMs (Fig. 1C).

To investigate whether stratification of the Swiss 3T3 cell sheet could promote hepatic maturation of the hEHs, hESCs (H9) were differentiated into the hepatocyte-like cells according to the protocol described in Fig. 1A, and then the gene expression levels of hepatocyte-related markers and the amount of albumin (ALB) secretion in the hEHs-Swiss were measured on day 25 (Fig. 2). By 3D co-culturing of the hepatocyte-like cells with the Swiss 3T3 cell sheet for 10 days (days 15–25), the gene expression levels of hepatocyte-related markers, such as *ALB* (Fig. 2A), *hepatocyte nuclear factor 4 alpha* (*HNF4A*) (Fig. 2B), cytochrome P450 (CYP) enzymes (*CYP2C9*, *CYP7A1*, *CYP1A2*, and *CYP3A5*) (Fig. 2D–G), and conjugating enzymes (*glutathione S-transferase alpha 1* [*GSTA1*], *GSTA2*, and *UDP glucuronosyltransferase* [*UGT1A1*]) (Fig. 2H–J) were significantly increased as compared with those in hEHs-mono. Moreover, the amount of ALB secretion in hEHs-Swiss was also up-regulated as compared with that in hEHs-mono (Fig. 2K). Because it is known that hepatoblasts can differentiate into hepatocytes and cholangiocytes [34,35], we examined the gene expression level of *cytokeratin 7* (*CK7*), a cholangiocyte-related marker, in hEHs-Swiss and hEHs-mono. In 3D co-culture with the Swiss 3T3 cell sheet, the gene expression level of *CK7* was down-regulated in the hEHs-Swiss relative to the hEHs-mono (Fig. 2C). These results clearly showed that stratification of the Swiss 3T3 cell sheet could promote the hepatic maturation of the hEHs and, in turn, suppress the cholangiocyte differentiation.

In order to investigate whether stratification of the Swiss 3T3 cell sheet promotes maturation of hiPHs as well as hEHs, the hiPSCs (Tic and 201B7) were differentiated into the hepatocyte-like cells according to the protocol described in Fig. 1A. The results showed that the gene expression levels of *ALB*, *CYP2C9*, *CYP3A5*, *CYP1A2*, and *GSTA1* in the hiPHs stratified with the Swiss 3T3 cell sheet (hiPHs-Swiss) were up-regulated in comparison with those in the monolayer hiPHs (hiPHs-mono) (Fig. 3A–E). Moreover, the gene expression level of *CK7* was markedly decreased in hiPHs-Swiss (Fig. 3F). The gene expression level of *ALB* in the hiPHs-Swiss differentiated from Tic was higher than that in the hiPHs-Swiss differentiated from 201B7, while the gene expression levels of CYP enzymes in the hiPHs-Swiss differentiated from Tic were lower than those in the hiPHs-Swiss differentiated from 201B7 (Fig. 3A–D). These results showed that stratification of the Swiss 3T3 cell sheet promoted hepatic maturation of both hEHs and hiPHs.

3.2. Identification of maturation factors synthesized from Swiss 3T3 cells

The data described above indicate that hepatic maturation factors were produced in Swiss 3T3 cells. To elucidate the Swiss 3T3 cell-derived hepatic maturation factors, the hEHs were cultured in cell culture-insert systems (insert-cultured), in which the hEHs were co-cultured with Swiss 3T3 cells without physical contacts, or co-cultured with Swiss 3T3 cells. Quantitative PCR analysis revealed that the gene expression levels of *ALB* and *CYP2C9* in the insert-cultured hEHs were increased in comparison with the hEHs-mono, while the expression levels of these genes were lower than

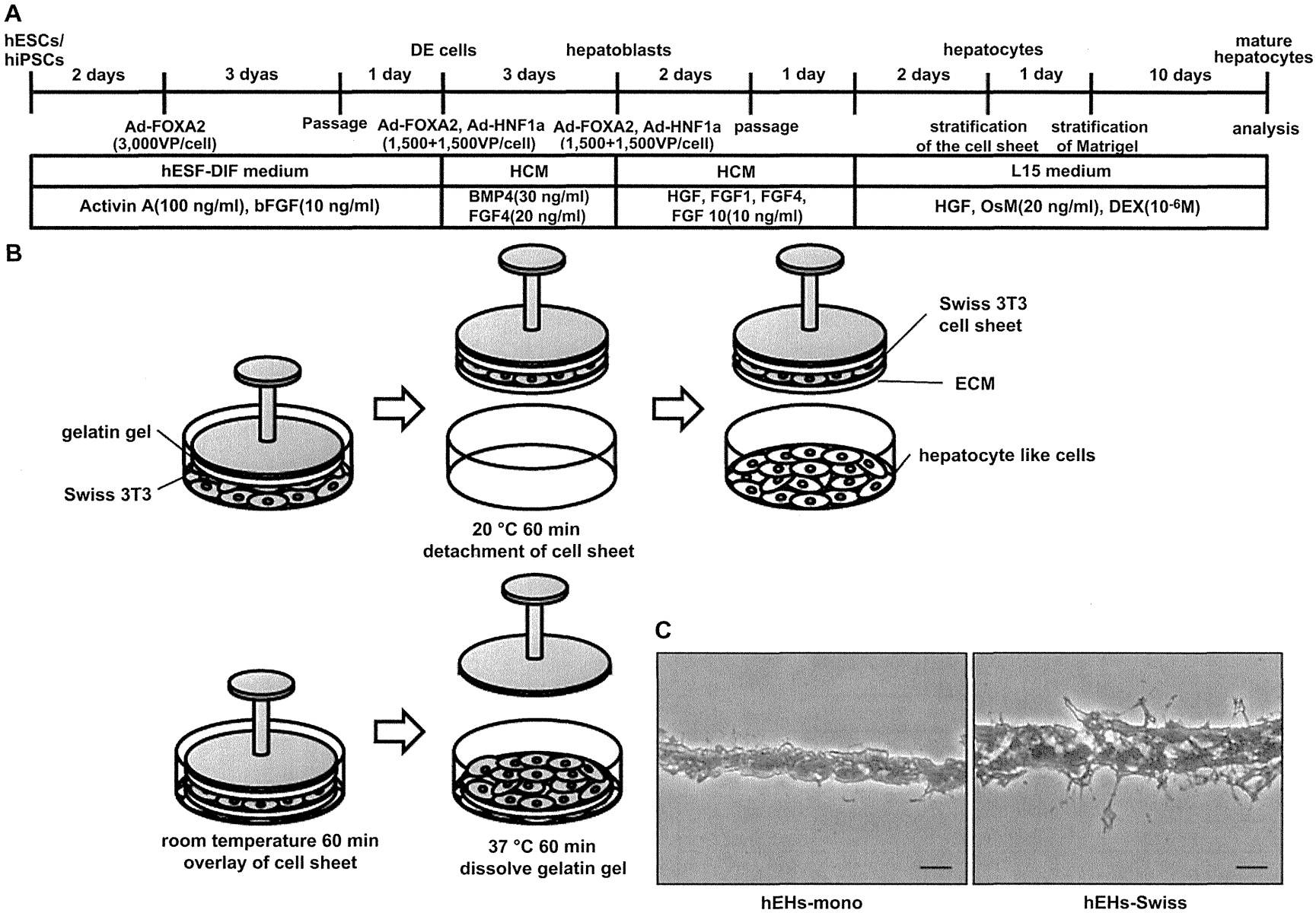

Fig. 1. Experimental protocol and schematic illustration of the procedure to stratify Swiss 3T3 cells on hepatocyte-like cells. (A) The procedure for hepatic differentiation of human embryonic stem cells (hESCs) and human induced pluripotent stem cells (hiPSCs) using stratification of the Swiss 3T3 cell sheet. Details of the hepatic differentiation procedure are described in the Materials and methods section. (B) The stratifying protocol was performed by using gelatin-coated manipulator. Details of the stratifying procedure are described in the Materials and methods section. (C) Phase-contrast micrographs of the vertical sections with monolayer hESC (H9)-derived hepatocyte-like cells (hEHs-mono) or hepatocyte-like cells stratified with Swiss 3T3 cell sheet (hEHs-Swiss) on day 15. Scale bars represent 25 μM.

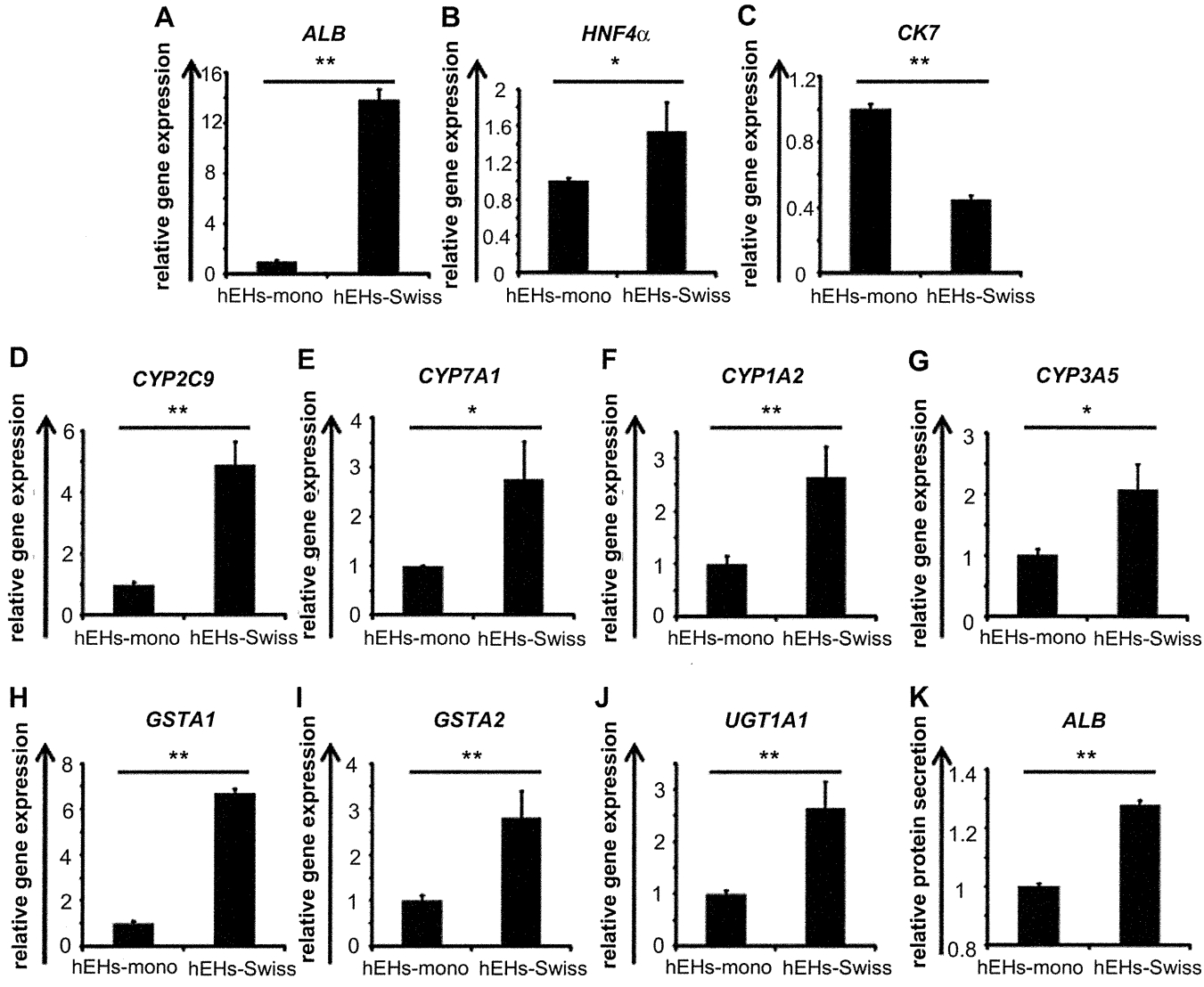

Fig. 2. Stratification of Swiss 3T3 cell sheet on hEHs promotes hepatic maturation. hESCs (H9) were differentiated into hepatocyte-like cells as described in Fig. 1A. (A–K): On day 25, the gene expression levels of *ALB* (A), *HNF4A* (B), *CK7*(C), *CYP2C9* (D), *CYP7A1* (E), *CYP1A2* (F), *CYP3A5* (G), *GSTA1* (H), *GSTA2* (I), and *UGT1A1* (J) were examined in monolayer hESC-derived hepatocyte-like cells (hEHs-mono) and hESC-derived hepatocyte-like cells stratified with Swiss 3T3 cell sheet (hEHs-Swiss) by real-time RT-PCR. The values were graphed as the fold-changes relative to hEHs-mono. (K) On day 25, the amounts of ALB secretion were examined in hEHs-mono or hEHs-Swiss by ELISA. The values were graphed as the fold-changes relative to hEHs-mono. All data are represented as means ± Standard Deviation (SD) ($n = 3$). *$P < 0.05$ **$P < 0.01$.

those in the co-cultured hEHs (Fig. 4A and B). Furthermore, a significant elevation of *CYP1A2* and *CYP3A5* gene expression was observed only in the co-cultured hEHs (Fig. 4C and D). Therefore, these data indicate that physical contacts between hEHs and Swiss 3T3 cells play an important role in hepatic maturation of the hEHs, although Swiss 3T3 cell-derived soluble factors also played a small role in the hepatic maturation.

Because ECMs are important factors in hepatic differentiation [36], we examined the effect of Swiss 3T3 cell-derived ECMs on hepatic maturation of the hEHs. Swiss 3T3 cells abundantly synthesize collagen and almost all of the synthesized collagen is type I collagen [37]. To mimic 3D co-culture with Swiss 3T3 cell sheet, type I collagen gel was stratified onto the hEHs. As a control, Matrigel, which contains abundant type IV collagen but not type I collagen, was stratified onto the hEHs. As with the case of the Swiss 3T3 cell sheet stratification, the hEHs-mono stratified with type I collagen gel showed an elevation of hepatocyte-related marker, but a reduction of cholangiocyte marker (Fig. 5A and B, hEHs-mono). In addition, stratification of type I collagen augmented the hepatic maturation of the Swiss 3T3 cell sheet-stratified hEHs (Fig. 5A and B, hEHs-Swiss). We further examined the role of Swiss 3T3 cell-derived type I collagen on hepatic maturation using 2,2′-Bipyridyl, an inhibitor of collagen synthesize. The collagen synthesis in Swiss 3T3 cells could be efficiently inhibited by treatment with 2,2′-Bipyridyl, as determined by Western blotting analysis (Fig. 5C). Quantitative RT-PCR analysis revealed that the gene expression level of *ALB* was significantly down-regulated, but that of CK7 was up-regulated in the hEHs-Swiss cultured in the presence of 2,2′-Bipyridyl (Fig. 5D and E). Taken together, our findings indicated that type I collagen, which was synthesized from Swiss 3T3 cells, was indispensable for the maturation of the hEHs by Swiss 3T3 cell sheet.

4. Discussion

Our main purpose in the current study was to develop a more efficient method for hepatic maturation of the hEHs and hiPHs, because such a method will be needed to generate more mature hepatocyte-like cells, which have potent activity to metabolize drugs, for wide-spread use of drug screening. Therefore, we

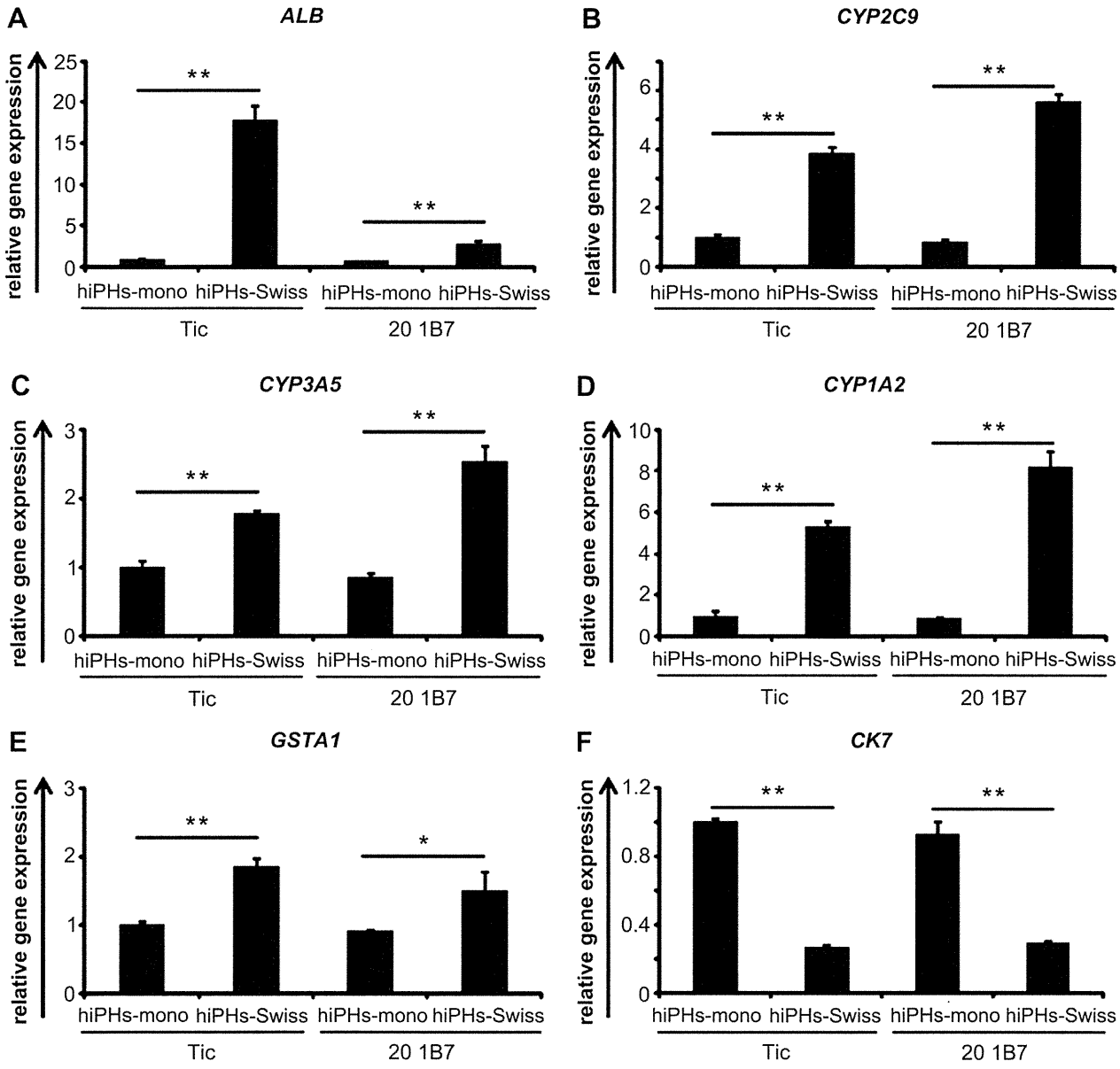

Fig. 3. Stratification of Swiss 3T3 cell sheet on hiPHs promotes hepatic maturation. Human induced pluripotent stem cells (hiPSCs) (Tic and 201B7) were differentiated into hepatocyte-like cells as described in Fig. 1A. (A–F): On day 25, the gene expression levels of *ALB* (A), *CYP2C9* (B), CYP3A5(C), *CYP1A2* (D), *GSTA1* (E), and *CK7* (F) were examined in monolayer hiPSC-derived hepatocyte-like cells (hiPHs-mono) and hiPSC-derived hepatocyte-like cells stratified with Swiss 3T3 cell sheet (hiPHs-Swiss) by real-time RT-PCR. The values were graphed as the fold-changes relative to hiPHs-mono differentiated from Tic. All data are represented as means ± SD ($n = 3$). $^{*}P < 0.05$ $^{**}P < 0.01$.

attempted to employ a cell sheet engineering technology to further induce maturation of the hEHs and hiPHs.

We observed a significant increase in the expression of hepatocyte-related genes in the hEHs- and hiPHs-Swiss as compared with those in the hEHs- and hiPHs-mono, respectively (Figs. 2 and 3), indicating that 3D co-culture with the Swiss 3T3 cell sheet was effective to promote hepatic maturation of the hEHs and hiPHs. On the other hand, Han et al. have recently shown that hESC-derived DE cells cannot be promoted to differentiate into hepatoblasts by co-culture of mouse fibroblast 3T3 cells [38]. Considering that primary rat hepatocytes are also able to grow and retain their functions for a long period of time in the presence of Swiss 3T3 cells [19,20], Swiss 3T3 cells would probably have the capacity to support the functions of freshly isolated mature hepatocytes and hESC- or hiPSC-derived hepatocyte-like cells, but not DE cells. Besides Swiss 3T3 cells, we attempted to maturate the hEHs using 3D co-culture with the bovine carotid artery endothelial cell sheet, because Kim et al. recently succeeded in creating a functional hepatocyte culture system by stacking bovine carotid artery endothelial cell sheets on primary rat hepatocytes [25]. However, our preliminary data showed that Swiss 3T3 cell sheets were superior to the bovine carotid artery endothelial cell sheets in terms of hepatic maturation of hEHs (data not shown). Thus, we conducted the present experiments to facilitate hepatic differentiation of human pluripotent stem cells using Swiss 3T3 cell sheets.

Interestingly, we found a difference in hepatic differentiation efficiency among hiPSC lines (Fig. 3). This might have been due to epigenetic memory of the hiPSC line, because several studies showed that the epigenetic memory of iPSCs affected the differentiation capacity [39,40]. Kleger et al. showed that iPSCs generated from mouse liver progenitor cells, could be more effectively differentiated into hepatocyte-like cells in comparison with iPSCs

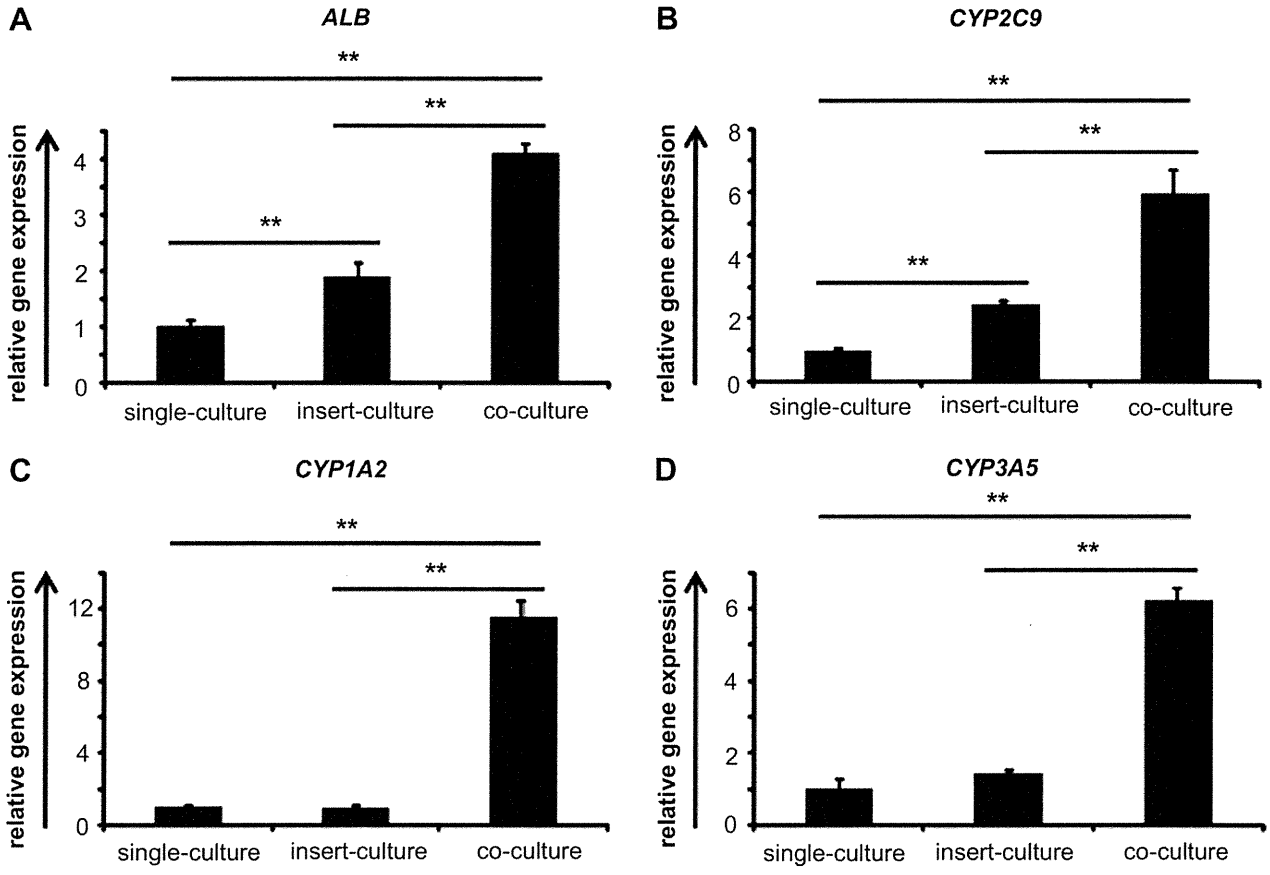

Fig. 4. Physical contacts between hESC-derived hepatocyte-like cells and Swiss 3T3 cells promote hepatic maturation. hESCs (H9) were differentiated into hepatocyte-like cells as described in Fig. 1A until day 14, and then the cells were differentiated into hepatocyte-like cells by single-culture, insert-culture, or co-culture with Swiss 3T3 cells. (A–D): On day 25, the gene expression levels of *ALB* (A), *CYP2C9* (B), *CYP1A2* (C) and *CYP3A5* (D) were examined in hESC-derived hepatocyte-like cells (hEHs) differentiated by single-culture, insert-culture, or co-culture with Swiss 3T3 cells by real-time RT-PCR. The values were graphed as the fold-changes relative to hEHs by single-culture. All data are represented as means ± SD ($n = 3$). $^{**}P < 0.01$.

generated from mouse embryo fibroblasts [41]. Thus, to more efficiently differentiate into hepatocyte-like cells from hiPSCs, it might be valuable to employ hiPSCs generated from freshly isolated human hepatocytes. Moreover, by using our 3D co-culture system, such hiPSCs would be differentiated into more mature hepatocyte-like cells.

We investigated the Swiss 3T3 cell-derived hepatic maturation factors by using cell culture inserts, and found that the physical contacts between Swiss 3T3 cells and the hEHs were the major factors contributing to the hepatic maturation of hEHs (Fig. 4). Because Swiss 3T3 cell-derived soluble factors partially induce maturation of hEHs (Fig. 4A and B), it would also be interesting to search for hepatic maturation factors secreted from Swiss 3T3 cells.

To further investigate the maturation factors, we examined whether type I collagen, which is abundantly synthesized by Swiss 3T3 cells, could promote hepatic maturation. Stratification of type I collagen gel could lead to a promotion of hepatic maturation of hEHs-mono as well as hEHs-Swiss (Fig. 5A). We also found that hepatic maturation by 3D co-culture with the Swiss 3T3 cell sheet was suppressed by inhibition of collagen synthesis (Fig. 5D). Taken together, these results show that type I collagen is one of the key molecules in promotion of hepatic maturation by stratification of Swiss 3T3 cells. It is known that the space of Disse, which faces hepatocytes directly, contains various kinds of ECM proteins, including type I collagen [42]. Because the conditions in 3D co-culture, which contains type I collagen synthesized from Swiss 3T3 cells, can mimic the *in vivo* liver microstructure, including the space of Disse, the hepatic maturation from hEHs and hiPHs might be efficiently promoted. Furthermore, it was also reported that, by the stratification of type I collagen gel in primary rat hepatocyte culture, the cytoskeletal organizations, such as actin localization, in primary rat hepatocytes were changed and stress fibers were obliterated just as in the *in vivo* state [43]. They also showed that the stratification of type I collagen gel in primary rat hepatocyte culture maintained ALB secretion in primary rat hepatocyte. Thus, the alteration of the cytoskeletal organization might also be changed in the hEHs and hiPHs by 3D co-culture with the Swiss 3T3 cell sheet. For these reasons, it could be speculated that stratification of Swiss 3T3 cell sheets positively affects the maturation process of hEHs and hiPHs mediated by cell-to-cell and cell-type I collagen–cell interactions. The expression level of the *CK7* gene in the hEHs was down-regulated by stratification of the Swiss 3T3 cell sheet or type I collagen gel (Figs. 2C and 5B). Although Matrigel, which contains large amount of type IV collagen, is widely used to differentiate hESCs and hiPSCs into hepatocyte-like cells, it is reported that type IV collagen promotes cholangiocyte differentiation [44]. Therefore, it would be important to note that stratification of Swiss 3T3 cell sheet inhibits the cholangiocyte differentiation and thereby allows the cells to drive the way to hepatic differentiation. Although we showed that a Swiss 3T3 cell-derived type I collagen plays an important role in hepatic maturation, it was likely that the other soluble factors would also be involved in the promotion of hepatic maturation.

We employed Swiss 3T3 cells for 3D co-culture with the hEHs and hiPHs. However, it would be an attractive study to employ other kinds of cells such as liver sinusoidal endothelial cells, stellate

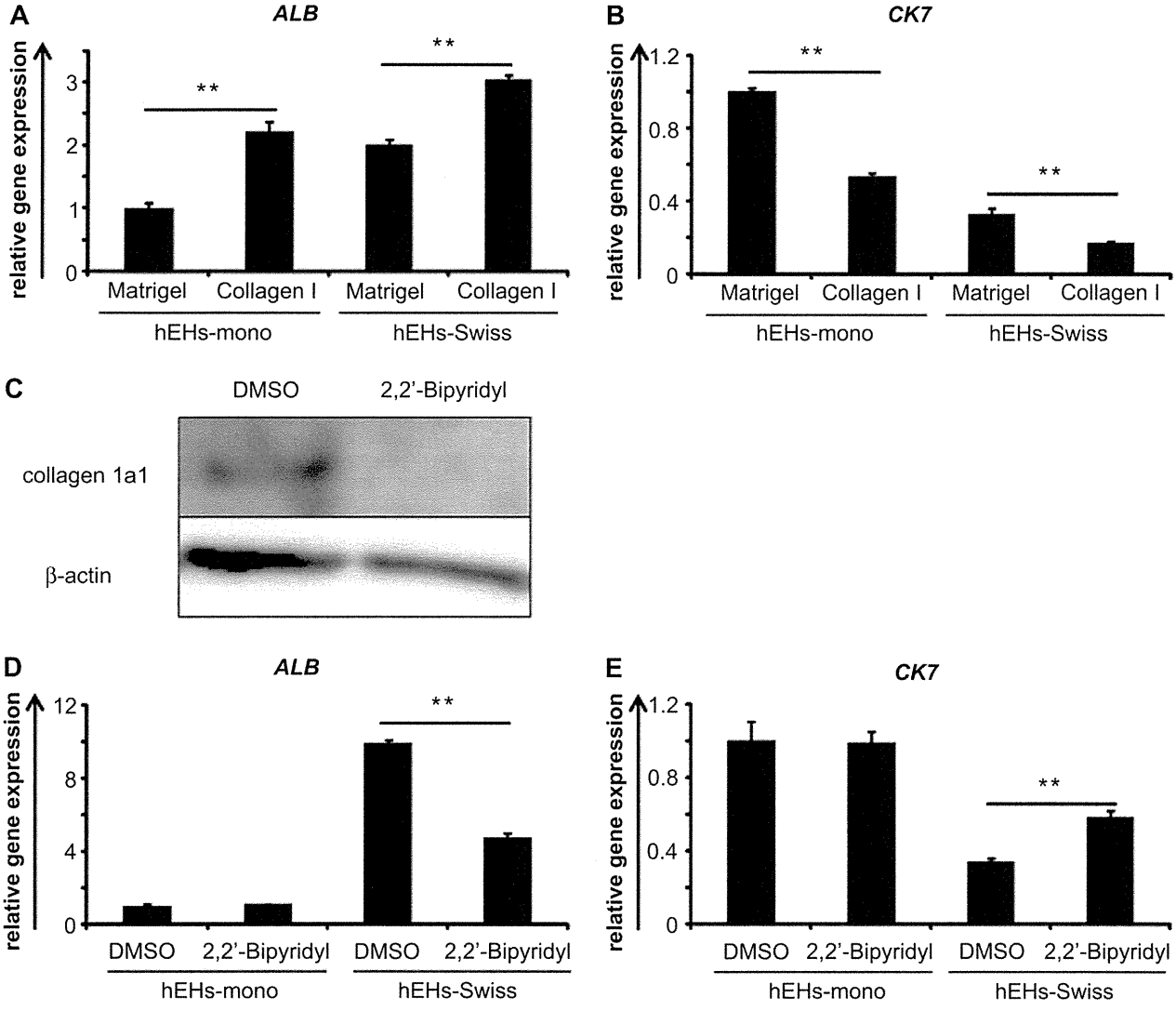

Fig. 5. Stratification of type I collagen gel promotes hepatic maturation. (A and B) hESCs (H9) were differentiated into hepatocyte-like cells as described in Fig. 1A until day 14, and then type I collagen gel (collagen I) or Matrigel are stratified on monolayer hESC-derived hepatocyte-like cells (hEHs-mono) and hESC-derived hepatocyte-like cells stratified with Swiss 3T3 cell sheet (hEHs-Swiss). On day 25, the gene expression levels of *ALB* (A) and *CK7* (B) were examined in hEHs-mono and hEHs-Swiss cultured with Matrigel or type I collagen gel by real-time RT-PCR. (C) Swiss 3T3 cells were cultured with 2,2′-Bipyridyl or solvent (0.1% DMSO) for 3 days, and then the expression of type I collagen precursor, col1a1, in these cells were detected by Western blot analysis. (D and E) hESCs (H9) were differentiated into hepatocyte-like cells as described in Fig. 1A. After stratification of Swiss 3T3 cells on day 14, these cells were treated with 2,2′-Bipyridyl or solvent (0.1% DMSO). On day 25, the gene expression levels of *ALB* (D) and *CK7* (E) were examined in hEHs-mono and hEHs-Swiss treated with 2,2′-Bipyridyl or solvent (0.1% DMSO) by real-time RT-PCR. The values were graphed as the fold-changes relative to hEHs-mono cultured with Matrigel. All data are represented as means ± SD ($n = 3$). $^{**}P < 0.01$.

cells, and Kupffer cells, to mimic the *in vivo* liver microstructure. By mimicking the *in vivo* liver microstructure, basic molecular mechanisms, including cell–cell interactions, in liver development would be clarified. Moreover, because our cell sheet technology allows us to stratify the multiple cell sheets and create layered 3D tissue constructs, combinations with multiple layers consisting of various types of cells might be able to develop an efficient method for hepatic maturation of the hEHs and hiPHs. In addition, by using new biomaterials with cell patterning techniques, more mature hepatocyte-like cells would be probably generated from human pluripotent stem cells, and thereby accelerate the research into tissue generation.

5. Conclusions

We succeeded in promoting the hepatic maturation of both the hEHs and hiPHs by stratification of the Swiss 3T3 cell sheet using a cell sheet engineering technology. We also determined that type I collagen, which is synthesized in Swiss 3T3 cells, plays an important role in hepatic maturation. Since our cell sheet engineering technology enables us to stratify multiple cell sheets, this technology would have the potential to mimic the *in vivo* liver microstructure and to generate hepatocyte-like cells, which have functions similar to primary hepatocytes. Our methods would be powerful tools for *in vitro* applications, such as drug toxicity screening in the early phase of pharmaceutical development.

Acknowledgements

We thank Misae Nishijima, Miki Yoshioka, Nobue Hirata, and Hiroko Matsumura for their excellent technical support. We also thank Tetsutaro Kikuchi (Cell Seed Inc) for providing a cell sheet stamp manipulator system. HM, KK, MKF, and TH were supported by grants from the Ministry of Health, Labor, and Welfare of Japan

(MEXT). HM was also supported by Japan Research foundation For Clinical Pharmacology and The Uehara Memorial Foundation. KO was supported by Special Coordination Funds for Promoting Science and Technology from MEXT. FS was supported by Program for Promotion of Fundamental Studies in Health Sciences of the National Institute of Biomedical Innovation (NIBIO).

Appendix A. Supplementary data

Supplementary data associated with this article can be found, in the online version, at doi:10.1016/j.biomaterials.2012.03.011.

References

[1] Thomson JA, Itskovitz-Eldor J, Shapiro SS, Waknitz MA, Swiergiel JJ, Marshall VS, et al. Embryonic stem cell lines derived from human blastocysts. Science 1998;282:1145–7.
[2] Takahashi K, Tanabe K, Ohnuki M, Narita M, Ichisaka T, Tomoda K, et al. Induction of pluripotent stem cells from adult human fibroblasts by defined factors. Cell 2007;131:861–72.
[3] Duan Y, Catana A, Meng Y, Yamamoto N, He S, Gupta S, et al. Differentiation and enrichment of hepatocyte-like cells from human embryonic stem cells in vitro and in vivo. Stem Cells 2007;25:3058–68.
[4] Touboul T, Hannan NR, Corbineau S, Martinez A, Martinet C, Branchereau S, et al. Generation of functional hepatocytes from human embryonic stem cells under chemically defined conditions that recapitulate liver development. Hepatology 2010;51:1754–65.
[5] Brolen G, Sivertsson L, Bjorquist P, Eriksson G, Ek M, Semb H, et al. Hepatocyte-like cells derived from human embryonic stem cells specifically via definitive endoderm and a progenitor stage. J Biotechnol 2010;145:284–94.
[6] Cai J, Zhao Y, Liu Y, Ye F, Song Z, Qin H, et al. Directed differentiation of human embryonic stem cells into functional hepatic cells. Hepatology 2007;45:1229–39.
[7] Snykers S, De Kock J, Rogiers V, Vanhaecke T. In vitro differentiation of embryonic and adult stem cells into hepatocytes: state of the art. Stem Cells 2009;27:577–605.
[8] Kamiya A, Kinoshita T, Miyajima A. Oncostatin M and hepatocyte growth factor induce hepatic maturation via distinct signaling pathways. FEBS Lett 2001;492:90–4.
[9] Si-Tayeb K, Lemaigre FP, Duncan SA. Organogenesis and development of the liver. Dev Cell 2010;18:175–89.
[10] Duan Y, Ma X, Zou W, Wang C, Bahbahan IS, Ahuja TP, et al. Differentiation and characterization of metabolically functioning hepatocytes from human embryonic stem cells. Stem Cells 2010;28:674–86.
[11] Inamura M, Kawabata K, Takayama K, Tashiro K, Sakurai F, Katayama K, et al. Efficient generation of hepatoblasts from human ES cells and iPS cells by transient overexpression of homeobox gene HEX. Mol Ther 2011;19:400–7.
[12] Takayama K, Inamura M, Kawabata K, Katayama K, Higuchi M, Tashiro K, et al. Efficient generation of functional hepatocytes from human embryonic stem cells and induced pluripotent stem cells by HNF4alpha transduction. Mol Ther 2012;20:127–37.
[13] Takayama K, Inamura M, Kawabata K, Tashiro K, Katayama K, Sakurai F, et al. Efficient and directive generation of two distinct endoderm lineages from human ESCs and iPSCs by differentiation stage-specific SOX17 transduction. PLoS One 2011;6:e21780.
[14] Zaret KS. Liver specification and early morphogenesis. Mech Dev 2000;92:83–8.
[15] Matsumoto K, Yoshitomi H, Rossant J, Zaret KS. Liver organogenesis promoted by endothelial cells prior to vascular function. Science 2001;294:559–63.
[16] Kinoshita T, Sekiguchi T, Xu MJ, Ito Y, Kamiya A, Tsuji K, et al. Hepatic differentiation induced by oncostatin M attenuates fetal liver hematopoiesis. Proc Natl Acad Sci USA 1999;96:7265–70.
[17] Ohashi K, Yokoyama T, Yamato M, Kuge H, Kanehiro H, Tsutsumi M, et al. Engineering functional two- and three-dimensional liver systems in vivo using hepatic tissue sheets. Nat Med 2007;13:880–5.
[18] Yamasaki C, Tateno C, Aratani A, Ohnishi C, Katayama S, Kohashi T, et al. Growth and differentiation of colony-forming human hepatocytes in vitro. J Hepatol 2006;44:749–57.
[19] Sato H, Funahashi M, Kristensen DB, Tateno C, Yoshizato K. Pleiotrophin as a Swiss 3T3 cell-derived potent mitogen for adult rat hepatocytes. Exp Cell Res 1999;246:152–64.
[20] Hui EE, Bhatia SN. Micromechanical control of cell-cell interactions. Proc Natl Acad Sci USA 2007;104:5722–6.
[21] Khetani SR, Szulgit G, Del Rio JA, Barlow C, Bhatia SN. Exploring interactions between rat hepatocytes and nonparenchymal cells using gene expression profiling. Hepatology 2004;40:545–54.
[22] Abu-Absi SF, Hansen LK, Hu WS. Three-dimensional co-culture of hepatocytes and stellate cells. Cytotechnology 2004;45:125–40.
[23] Gu J, Shi X, Zhang Y, Chu X, Hang H, Ding Y. Establishment of a three-dimensional co-culture system by porcine hepatocytes and bone marrow mesenchymal stem cells in vitro. Hepatol Res 2009;39:398–407.
[24] Thomas RJ, Bhandari R, Barrett DA, Bennett AJ, Fry JR, Powe D, et al. The effect of three-dimensional co-culture of hepatocytes and hepatic stellate cells on key hepatocyte functions in vitro. Cells Tissues Organs 2005;181:67–79.
[25] Kim K, Ohashi K, Utoh R, Kano K, Okano T. Preserved liver-specific functions of hepatocytes in 3D co-culture with endothelial cell sheets. Biomaterials 2012;33:1406–13.
[26] Harimoto M, Yamato M, Hirose M, Takahashi C, Isoi Y, Kikuchi A, et al. Novel approach for achieving double-layered cell sheets co-culture: overlaying endothelial cell sheets onto monolayer hepatocytes utilizing temperature-responsive culture dishes. J Biomed Mater Res 2002;62:464–70.
[27] Yu YD, Kim KH, Lee SG, Choi SY, Kim YC, Byun KS, et al. Hepatic differentiation from human embryonic stem cells using stromal cells. J Surg Res 2011;170:e253–61.
[28] Tuleuova N, Lee JY, Lee J, Ramanculov E, Zern MA, Revzin A. Using growth factor arrays and micropatterned co-cultures to induce hepatic differentiation of embryonic stem cells. Biomaterials 2010;31:9221–31.
[29] Miki T, Ring A, Gerlach J. Hepatic differentiation of human embryonic stem cells is promoted by three-dimensional dynamic perfusion culture conditions. Tissue Eng Part C Methods 2011;17:557–68.
[30] Kawabata K, Sakurai F, Yamaguchi T, Hayakawa T, Mizuguchi H. Efficient gene transfer into mouse embryonic stem cells with adenovirus vectors. Mol Ther 2005;12:547–54.
[31] Maizel Jr JV, White DO, Scharff MD. The polypeptides of adenovirus. I. Evidence for multiple protein components in the virion and a comparison of types 2, 7A, and 12. Virology 1968;36:115–25.
[32] Furue MK, Na J, Jackson JP, Okamoto T, Jones M, Baker D, et al. Heparin promotes the growth of human embryonic stem cells in a defined serum-free medium. Proc Natl Acad Sci USA 2008;105:13409–14.
[33] Sasagawa T, Shimizu T, Sekiya S, Haraguchi Y, Yamato M, Sawa Y, et al. Design of prevascularized three-dimensional cell-dense tissues using a cell sheet stacking manipulation technology. Biomaterials 2010;31:1646–54.
[34] Lemaigre F, Zaret KS. Liver development update: new embryo models, cell lineage control, and morphogenesis. Curr Opin Genet Dev 2004;14:582–90.
[35] Zhao R, Duncan SA. Embryonic development of the liver. Hepatology 2005;41:956–67.
[36] Suzuki A. Role for growth factors and extracellular matrix in controlling differentiation of prospectively isolated hepatic stem cells. Development 2003;130:2513–24.
[37] Goldberg B. Collagen synthesis as a marker for cell type in mouse 3T3 lines. Cell 1977;11:169–72.
[38] Han S, Dziedzic N, Gadue P, Keller GM, Gouon-Evans V. An endothelial cell niche induces hepatic specification through Dual Repression of Wnt and Notch signaling. Stem Cells 2011;29:217–28.
[39] Kim K, Doi A, Wen B, Ng K, Zhao R, Cahan P, et al. Epigenetic memory in induced pluripotent stem cells. Nature 2010;467:285–90.
[40] Polo JM, Liu S, Figueroa ME, Kulalert W, Eminli S, Tan KY, et al. Cell type of origin influences the molecular and functional properties of mouse induced pluripotent stem cells. Nat Biotechnol 2010;28:848–55.
[41] Kleger A, Mahaddalkar P, Katz SF, Lechel A, Ju JY, Loya K, et al. Increased Reprogramming capacity of mouse liver progenitor cells, compared with differentiated liver cells, Requires BAF Complex. Gastroenterology, in press.
[42] Martinez-Hernandez A. The hepatic extracellular matrix. I. Electron immunohistochemical studies in normal rat liver. Lab Invest 1984;51:57–74.
[43] Dunn JC, Tompkins RG, Yarmush ML. Long-term in vitro function of adult hepatocytes in a collagen sandwich configuration. Biotechnol Prog 1991;7:237–45.
[44] Tanimizu N, Saito H, Mostov K, Miyajima A. Long-term culture of hepatic progenitors derived from mouse Dlk+ hepatoblasts. J Cell Sci 2004;117:6425–34.

Bioorganic & Medicinal Chemistry Letters 23 (2013) 503–506

Contents lists available at SciVerse ScienceDirect

Bioorganic & Medicinal Chemistry Letters

journal homepage: www.elsevier.com/locate/bmcl

2′-Fluoro-6′-methylene-carbocyclic adenosine phosphoramidate (FMCAP) prodrug: In vitro anti-HBV activity against the lamivudine–entecavir resistant triple mutant and its mechanism of action

Ravindra K. Rawal [a], Uma S. Singh [a], Satish N Chavre [a], Jianing Wang [a], Masaya Sugiyama [b], Wai Hung [a], Rajgopal Govindarajan [a], Brent Korba [c], Yasuhito Tanaka [b], Chung K. Chu [a,*]

[a] The University of Georgia, College of Pharmacy, Athens, GA 30602, USA
[b] Nagoya City University Graduate School of Medical Sciences, Nagoya 467 8601, Japan
[c] Georgetown University Medical Center, WA 20057, USA

ARTICLE INFO

Article history:
Received 28 September 2012
Accepted 8 November 2012
Available online 24 November 2012

Keywords:
Carbocyclic–nucleos(t)ide
Anti-HBV activity
Wild-type
Lamivudine–entecavir triple mutant
Drug-resistant mutants

ABSTRACT

Novel 2′-fluoro-6′-methylene-carbocyclic adenosine (FMCA) monophosphate prodrug (FMCAP) was synthesized and evaluated for its in vitro anti-HBV potency against a lamivudine–entecavir resistant clone (L180M + M204V + S202G). FMCA demonstrated significant antiviral activity against wild-type as well as lamivudine–entecavir resistant triple mutant (L180M + M204V + S202G). The monophosphate prodrug (FMCAP) demonstrated greater than 12-fold (12×) increase in anti-HBV activity without increased cellular toxicity. Mitochondrial and cellular toxicity studies of FMCA indicated that there is no significant toxicity up to 100 μM. Mode of action studies by molecular modeling indicate that the 2′-fluoro moiety by hydrogen bond as well as the Van der Waals interaction of the carbocyclic ring with the phenylalanine moiety of the polymerase promote the positive binding, even in the drug-resistant mutants.

The chronic HBV infection is strongly associated with liver diseases like chronic hepatic insufficiency, cirrhosis and hepatocellular carcinoma (HCC).[1] According to the World Health Organization (WHO), currently about 2 billion people world-wide have been infected with HBV and more than 350 million live with chronic infection. Acute or chronic outcomes of HBV infection are estimated to cause the deaths of 600,000 people worldwide every year.[2]

Currently, there are several nucleos(t)ide analogues available to treat chronic hepatitis B virus infection.[3–6] The major target of these drugs is to inhibit the viral reverse transcriptase (RT)/DNA polymerase, which is responsible for the synthesis of the minus-strand DNA. Although the currently used agents are well tolerated and effective in suppressing the viral replication for extended periods, the significant rate of virological relapse caused by drug resistance remains a critical issue.

Lamivudine (LVD) was first introduced as the orally active anti-HBV agent in 1998. Lamivudine profoundly suppresses HBV replication in patients with chronic hepatitis B infection; however, lamivudine-resistant HBV (LVDr) was isolated from a significant numbers of patients during the treatment with lamivudine. Currently, there are several antiviral options exist for these patients viz., to use adefovir or high dose (1.0 mg/day) of entecavir, or more recently tenofovir. However, this resulted in also the development of resistance mutants during the long term therapy. At present, entecavir is the most prescribed drug, and is recommended for patients with the wild-type as well as for those harboring adefovir and lamivudine-resistant strains. However, recent clinical studies by Tanaka and his co-workers suggested that the entecavir mutant in the lamivudine-resistant patients (L180M + M204V + S202G) causes a viral breakthrough: 4.9% of patients at baseline increases to 14.6%, 24% and 44.8% at weeks 48, 96 and 144, respectively.[7] Therefore, it is of great interest to discover novel anti-HBV agent, which is effective against lamivudine- and entecavir-resistant triple mutants (L180M + M204V + S202G).

The potency of a nucleos(t)ide analogue is determined by its ability to serve as a competitive inhibitor of the HBV polymerase relative to that of the natural substrate, the nucleotide triphosphate.[8] However, host cellular kinases limit the pharmacological potency of nucleoside analogues by phosphorylation to their corresponding triphosphates. Particularly, the initial kinase action on the nucleoside to the monophosphate is the rate-limiting step. However, many synthetic nucleosides are not phosphorylated or the rate of phosphorylation is very slow due to the structural requirement of the kinases, resulting in only generating a low quantity of the triphosphate. To overcome this phosphorylation issue, nucleoside phosphoramidate prodrugs have been introduced,[8,9] which

* Corresponding author. Address: Department of Pharmaceutical and Biomedical Sciences, College of Pharmacy, The University of Georgia, Athens, GA 30602, USA. Tel.: +1 706 542 5379; fax: +1 706 542 5381.
E-mail address: DCHU@rx.uga.edu (C.K. Chu).

0960-894X/$ - see front matter © 2012 Elsevier Ltd. All rights reserved.
http://dx.doi.org/10.1016/j.bmcl.2012.11.027

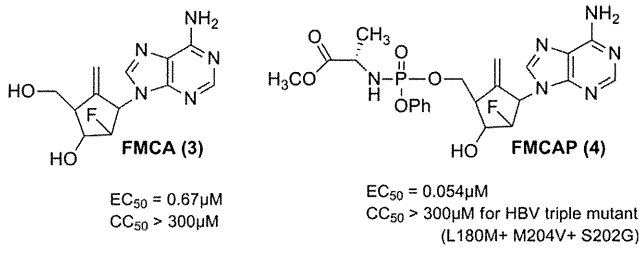

Figure 1. Structures of 2′-fluoro-6′-methylene-carbocyclic adenosine (FMCA; **3**) and its prodrug (FMCAP; **4**).

can bypass the rate-limiting first step of monophosphorylation. Phosphoramidate prodrugs have demonstrated to enhance the nucleoside potency in cell culture as well as in patients.[10,11] This methodology greatly increases the lipophilicity of the nucleotide to increase the cell penetration as well as to target the liver cells in vivo.

In this communication, we present that a FMCA phosphoramidate prodrug is such an agent, which can potentially be used for the treatment of patients who experience viral breakthrough due to the triple mutants caused by the use of lamivudine and entecavir.

In our previous report, we have demonstrated that the novel carbocyclic adenosine analog **3** (FMCA Fig. 1) exhibits significant anti-HBV activity against wild type as well as adefovir/lamivudine resistant strains.[12] The present study describes the synthesis and antiviral evaluation of a phosphoramidate of FMCA (FMCAP), which demonstrated the significantly improved in vitro potency. Additionally, we studied its mechanism of action how FMCA-TP can effectively bind to the HBV polymerase by molecular modeling and still exerts the antiviral activity against the lamivudine–entecavir triple mutant (L180M + M204V + S202G).

FMCAP (**4**, Scheme 1)[13] was synthesized using a known method in the literature,[14,15] in which the phosphorylation of phenol with phosphorus oxychloride generates phenyl dichlorophosphate **1**, which was coupled with L-alanine methyl ester in the presence of *tri*-ethyl amine in dichloromethane to give chlorophosphoramidate reagent **2**, which, in turn, was coupled with FMCA **3** in the presence of 1-methyl imidazole in THF to furnish the phosphoramidate **4** in good yield.

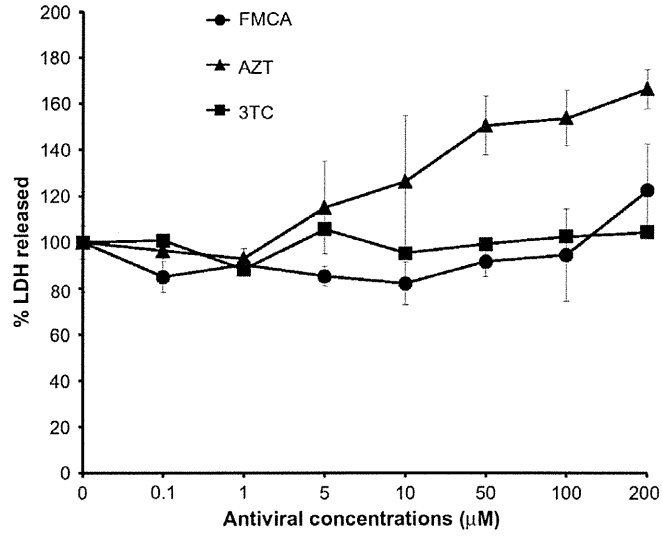

Figure 2. Mitochondrial toxicity of FMCA **3**, AZT and 3TC through lactate dehydrogenase release (LDH) assay.

FMCA **3** and FMCAP **4** were evaluated in vitro against the wild-type as well as the lamivudine–entecavir resistant clone (L180M + S202I + M202V). The FMCA **3** and FMCAP **4** demonstrated significant anti-HBV activity (EC_{50} 0.548 ± 0.056 & 0.062 ± 0.011 μM, respectively) against the wild-type virus, while lamivudine and entecavir also demonstrated potent anti-HBV activity (EC_{50} 0.056 ± 0.003 & 0.008 μM, respectively) (Table 1). It is noteworthy to mention that the anti-HBV potency of FMCAP (**4**) was increased to eight-fold (8×) in comparison to that of FMCA **3**, which indicates the importance of the initial phosphorylation of the nucleoside.

FMCA **3** and FMCAP **4** were further evaluated for their in-vitro antiviral potency against a lamivudine–entecavir resistant clone (L180M + M204V + S202G). It was observed that the anti-HBV potency of both FMCA **3** and FMCAP **4** (EC_{50} 0.67 & 0.054 μM, respectively) were maintained against the resistant clone, and furthermore, the anti-HBV activity of FMCAP **4** was enhanced a 12-fold (12×) with respect to that of FMCA without significant enhancement of cellular toxicity. It was also noteworthy to mention that the anti-HBV potency of entecavir against the mutant

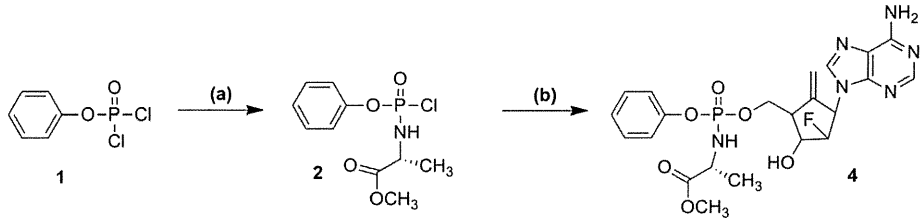

Scheme 1. Reagent and conditions: (a) L-alanine methyl ester hydrochloride, Et_3N, CH_2Cl_2; (b) FMCA (3), NMI, THF, rt overnight.

Table 1
In vitro anti-HBV activity of FMCA **3**, FMCAP **4**, lamivudine and entecavir against wild-type and entecavir drug-resistant mutant (L180M + M204V + S202G) in Huh7 cells

Compounds	HBV Strains			
	Wild-type			L180M + M204V + S202G
	EC_{50} (μM)	EC_{90} (μM)	CC_{50} (μM)	EC_{50} (μM)
FMCA **3**	0.548 ± 0.056	6.0 ± 0.400	>300	0.67
FMCAP **4**	0.062 ± 0.011	0.46 ± 0.060	>300	0.054
Lamivudine	0.056 ± 0.003	0.142 ± 0.008	>300	>500[17]
Entecavir	0.008	0.033	28	1.20[16]

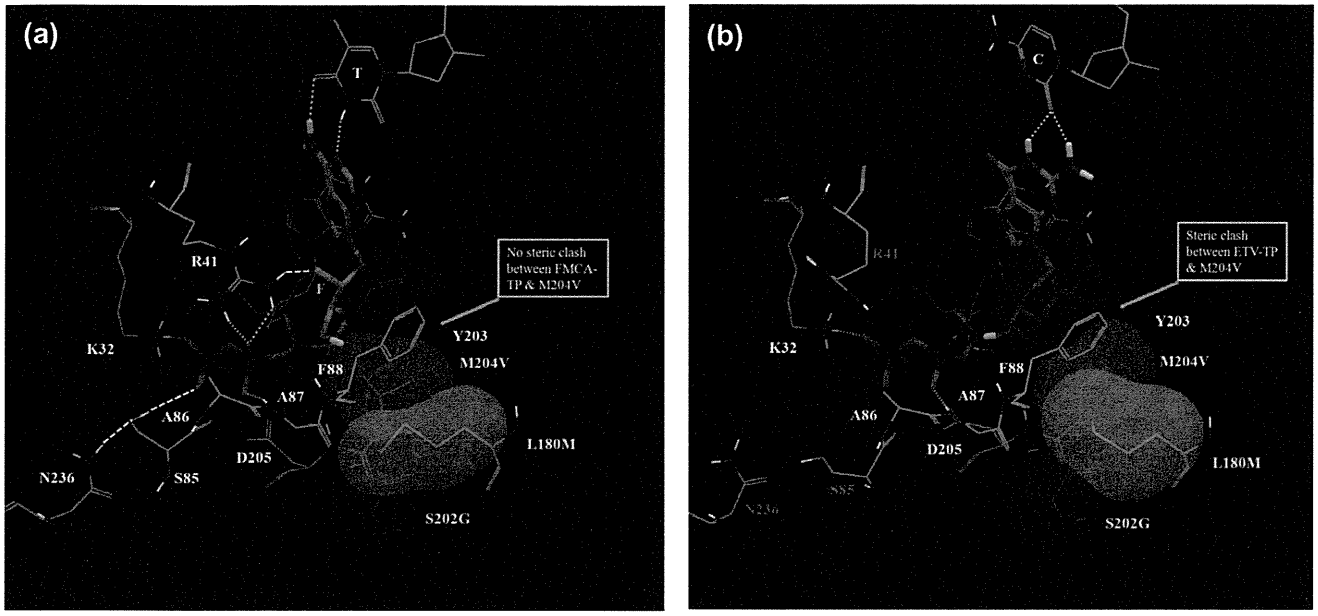

Figure 3. (a) FMCA-TP binding mode in ETVr (L180M + M204V + S202G); and (b) ETV-TP binding mode in ETVr (L180M + M204V + S202G) and there is a steric hindrance. Yellow dotted lines are hydrogen bonding interactions (<2.5 Å). The Van der Waals surface of L180M is colored yellow. The Van der Waals surface of M204V is shown in spring green. The Van der Waals surface of S202G is colored orange. The exocyclic double bond is shown blue color.

Table 2
MBAE (multi-ligand bimolecular association with energetics) calculation of FMCA-TP and ETV-TP after Glide XP docking[21] and energy minimization[22]

Strains	Compounds	Energy difference results (ΔE, kcal/mol)		
		Total energy	VdW[a]	Electrostatic
Wild-type	FMCA-TP	−588.05	375.78	−6341.08
	ETV-TP	−597.25	350.35	−6009.65
ETVr	FMCA-TP	−591.54	359.91	−6245.68
(L180M + M204V + S202G)	ETV-TP	−320.28	248.82	−4831.12

[a] Van der Waals interaction.

was reduced by 150-fold (EC_{50} 1.2 μM) in comparison to wild type.[16]

In the preliminary mitochondrial toxicity studies in HepG2 cells by measuring the lactic dehydrogenase release,[18] FMCA **3** did not exhibit any significant toxicity up to 100 μM like lamivudine (3TC), while azidothymidine (AZT) shows the increase of toxicity (Fig. 2).

In our previous report, we described molecular modeling studies for favorable anti-HBV activity of FMCA-TP in wild-type as well as in N236T adefovir resistant (ADVr) mutant.[12] In the current studies, it was of interest to know how the FMCA and its prodrug maintain the anti-HBV activity against ETVr triple mutant (L180M + M204V + S202G) in comparison to entecavir. Therefore, molecular modeling studies were conducted to obtain the insight of the molecular mechanism of FMCA-TP by using the Schrodinger Suite modules.[19] A previously described homology model was used to further explore the impact of the ETVr to the HBV-RT.[12] The homology model of HBV-RT was constructed based on the published X-ray crystal structure of HIV reverse transcriptase (PDB code: 1RTD).[20]

The binding mode of FMCA-TP and ETV-TP in ETVr (L180M + M204V + S202G) HBV-RT are depicted in Figure 3a and b, respectively. Their MBAE (multi-ligand biomolecular association with energetics)[22] calculations of FMCA-TP (total energy, wt −588.05 & ETVr −591.54 kcal/mol) and ETV-TP (total energy, wt −597.25 & ETVr −320.28 kcal/mol) after glide XP (extra precision) docking[21] and energy minimization in ETVr HBV-RT are shown in Table 2. The triphosphate of FMCA-TP forms all the network of hydrogen bonds with the active site residues (Fig. 3a), K32, R41, S85 & A87 in the similar manner as in wild-type,[12] whereas ETV-TP lose the hydrogen bonding with R41 & S85. The γ-phosphate of FMCA-TP maintains a critical H-bonding with the OH of S85 with connection of hydrogen bonds between S85 and N236 in ETVr HBV-RT also. However, γ-phosphate ETV-TP does not maintain this critical H-bonding with S85 and N236 (Fig. 3b).

The carbocyclic ring with an exocyclic double bond of FMCA-TP and ETV-TP makes the favorable Van der Waals interaction with F88 in ETVr HBV-RT (Fig. 3a and b). There is no steric clash in between exocyclic double bond of FMCA-TP and M204V residue, whereas ETV-TP exocyclic double bond has steric clash with M204V residue in ETVr HBV-RT. The 2′-fluorine substituent in the carbocyclic ring of FMCA-TP appears to promote an additional binding with the NH of R41 guanidino group as shown in Figure 3a, which is in agreement with the antiviral activity of FMCA-TP shown in Table 1. Overall, the modeling studies can qualitatively explain the favorable anti-HBV activity of FMCA-TP against ETVr mutant (L180M + M204V + S202G) in comparison to entecavir as shown in Table 1.

In conclusion, 2′-fluoro-6′-methylene-carbocyclic adenosine phosphoramidate prodrug (FMCAP) was synthesized, which demonstrated the significantly increased anti-HBV potency relative to the parent compound, FMCA in vitro. Molecular modeling studies delineated the mechanism of FMCA-TP and how it can effectively bind to the lamivudine–entecavir resistant triple mutant resulting

in maintaining the anti-HBV activity against the mutant. Furthermore, FMCA has been studied for the release of lactic dehydrogenase for potential mitochondrial toxicity and found that no significant increase of toxicity of FMCA compared with other commonly used anti-HIV nucleoside drugs. Very recently, a preliminary in vivo study in chimeric mice harboring the triple mutant, FMCAP was found to reduce HBV viral load while entecavir did not (data not shown). In view of these promising anti-HBV activities and non-toxicity of FMCAP as well as the interesting mechanism of antiviral activity, the chiral synthesis of FMCAP and its mitochondrial toxicity studies for preclinical investigation are warranted.

Acknowledgment

This research was supported by the U.S. Public Health Service Grant AI-25899 (C.K.C.), NOI-AI-30046 (B.K.) from the National Institute of Allergy and Infectious Diseases, NIH.

References and notes

1. El-Serag, H. B. *N. Engl. J. Med.* **2011**, *365*, 1118.
2. http://www.who.int/mediacentre/factsheets/fs204/en/.
3. Sharon, A.; Jha, A. K.; Chu, C. K. *Analogue-Based Drug Discovery II*, 383.
4. Jarvis, B.; Faulds, D. *Drugs* **1999**, *58*, 101.
5. Marcellin, P.; Chang, T.; Lim, S. G.; Tong, M. J.; Sievert, W.; Shiffman, M. L.; Jeffers, L.; Goodman, Z.; Wulfsohn, M. S.; Xiong, S.; Fry, J.; Brosgart, C. L. *N. Engl. J. Med.* **2003**, *348*, 808.
6. Pol, S.; Lampertico, P. *J. Viral Hepat.* **2012**, *19*, 377.
7. Mukaide, M.; Tanaka, Y.; Shin, T.; Yuen, M. F.; Kurbanov, F.; Yokosuka, O.; Sata, M.; Karino, Y.; Yamada, G.; Sakaguchi, K. *Antimicrob. Agents Chemother.* **2010**, *54*, 882.
8. Hecker, S. J.; Erion, M. D. *J. Med. Chem.* **2008**, *51*, 2328.
9. Sofia, M. J.; Bao, D.; Chang, W.; Du, J.; Nagarathnam, D.; Rachakonda, S.; Reddy, P. G.; Ross, B. S.; Wang, P.; Zhang, H.-R.; Bansal, S.; Espiritu, C.; Keilman, M.; Lam, A. M.; Steuer, H. M. M.; Niu, C.; Otto, M. J.; Furman, P. A. *J. Med. Chem.* **2010**, *53*, 7202.
10. Chang, W.; Bao, D.; Chun, B.-K.; Naduthambi, D.; Nagarathnam, D.; Rachakonda, S.; Reddy, P. G.; Ross, B. S.; Zhang, H.-R.; Bansal, S.; Espiritu, C. L.; Keilman, M.; Lam, A. M.; Niu, C.; Steuer, H. M.; Furman, P. A.; Otto, M. J.; Sofia, M. J. *ACS Med. Chem. Lett.* **2010**, *2*, 130.
11. McGuigan, C.; Gilles, A.; Madela, K.; Aljarah, M.; Holl, S.; Jones, S.; Vernachio, J.; Hutchins, J.; Ames, B.; Bryant, K. D.; Gorovits, E.; Ganguly, B.; Hunley, D.; Hall, A.; Kolykhalov, A.; Liu, Y.; Muhammad, J.; Raja, N.; Walters, R.; Wang, J.; Chamberlain, S.; Henson, G. *J. Med. Chem.* **2010**, *53*, 4949.
12. Wang, J.; Singh, U. S.; Rawal, R. K.; Sugiyama, M.; Yoo, J.; Jha, A. K.; Scroggin, M.; Huang, Z.; Murray, M. G.; Govindarajan, R. *Bioorg. Med. Chem. Lett.* **2011**, *21*, 6328.
13. *Compound* **4**: ^{1}H NMR (500 Mz, *CDCl*$_3$) δ 8.35 (s, 1H), 7.86 (d, J = 3.0 Hz, 1H), 7.34–7.15 (m, 5H), 5.95 (m, 3H), 5.26 (d, J = 8.0 Hz, 1H), 5.01–4.90 (m, 1H), 4.83 (s, 1H), 4.50–4.41 (m, 2H), 4.25–4.04 (m, 3H), 3.71 (s, 3H), 3.07 (s, 1H), 1.40 (d, J = 6.5 Hz, 3 H); ^{19}F NMR (500 MHz, $CDCl_3$) δ −192.86 (m, 1F); ^{13}C NMR (125 MHz, *CDCl*$_3$) δ 171, 159.0, 156.5, 152.5, 150.4, 142.9, 130.1, 121.2, 120.3, 106.7, 102.4, 72.2, 71.1, 62.3, 51.9, 46.3, 43.9, 19.1; ^{31}P NMR (202 MHz, *CDCl*$_3$): δ 2.67, 2.99. Anal. Calcd For $C_{22}H_{26}FN_6O_6P.0.5H_2O$: C, 49.91; H, 5.14; N, 15.87; Found C, 49.84; H, 5.06; N, 15.22.
14. McGuigan, C.; Pathirana, R. N.; Mahmood, N.; Devine, K. G.; Hay, A. J. *Antiviral Res.* **1992**, *17*, 311.
15. Liang, Y.; Narayanasamy, J.; Schinazi, R. F.; Chu, C. K. *Bioorg. Med. Chem.* **2006**, *14*, 2178.
16. Walsh, A. W.; Langley, D. R.; Colonno, R. J.; Tenney, D. J. *PloS one* **2010**, *5*, e9195.
17. Villet, S.; Ollivet, A.; Pichoud, C.; Barraud, L.; Villeneuve, J. P.; Trépo, C.; Zoulim, F. *J. Hepatol.* **2007**, *46*, 531.
18. Lai, Y.; Tse, C. M.; Unadkat, J. D. *J. Biol. Chem.* **2004**, *279*, 4490.
19. Schrodinger Suite 2012; LLC, NY, 2012.
20. http://www.rcsb.org/pdb.
21. Glide version 5.8; Schrodinger LLC, NY, 2012.
22. Macromodel version 9.9; Schrodinger LLC, NY, 2012.

Replication of Hepatitis C Virus Genotype 3a in Cultured Cells

MOHSAN SAEED,[1] CLAIRE GONDEAU,[2] SUSU HMWE,[1] HIROSHI YOKOKAWA,[1,3] TOMOKO DATE,[1] TETSURO SUZUKI,[1] TAKANOBU KATO,[1] PATRICK MAUREL,[2] and TAKAJI WAKITA[1]

[1]*Department of Virology II, National Institute of Infectious Diseases, Tokyo, Japan;* [2]*Inserm U1040, Biotherapy Research Institute, Montpellier, France; and* [3]*Pharmaceutical Research Laboratories, Toray Industries, Inc., Kanagawa, Japan*

See Covering the Cover synopsis on page 1; see editorial on page 13.

Hepatitis C virus (HCV) genotype 3a is widespread worldwide, but no replication system exists for its study. We describe a subgenomic replicon system for HCV genotype 3a. We determined the consensus sequence of an HCV genome isolated from a patient, and constructed a subgenomic replicon using this clone. The replicon was transfected into HuH-7 cells and RNA replication was confirmed. We identified cell culture-adaptive mutations that increased colony formation multiple-fold. We have therefore established a genotype 3a replicon system that can be used to study this HCV genotype.

Keywords: Virology; Experimental Model; HCVGT3; In Vitro Culture System.

Hepatitis C virus (HCV) infection leads to chronic infection and advanced liver diseases in most infected adults.[1] Of the 6 major HCV genotypes, genotypes 1 and 2 are the most prevalent in North America, Europe, and Japan,[2,3] and are the most highly studied. However, other genotypes display specific characteristics. For example, genotype 3a infection can result in hepatic steatosis[4] and telaprevir and boceprevir are less effective against genotype 3a.[5] Therefore, the pathogenesis and inhibitor sensitivity of all HCV genotypes should be studied. Although HCV subgenomic replicons are useful for understanding viral/host factors involved in HCV replication and inhibitor sensitivity, only HCV replicons for genotypes 1a, 1b, and 2a have been established.[6–9] Here, we report on the robust genotype 3a replication system.

An almost complete HCV genome was recovered from the serum of a patient with post-transplantation recurrent HCV infection. This serum exhibited higher infectivity than other tested sera toward primary human hepatocytes (Supplementary Figure 1*A*). The isolate, named S310, contained the following structural elements: a 5′UTR (nt 1-339), an open reading frame encoding 3021 aa (nt 340-9402), and a 3′UTR (nt 9403-9654). Only the last 44 nt of the X-region (nt 9611-9654) could not be recovered. Two major virus populations were found; S310/A contained Ala, Thr, Thr, and Ile, and S310/B contained Thr, Ala, Ala, and Thr, at the 7th, 151st, 431st, and 472nd aa of the NS3 protein, respectively. S310 was clustered into genotype 3a by phylogenetic analysis (Supplementary Figure 1*B*). The complexity of the virus quasispecies in the serum was analyzed by sequencing the hypervariable region. Identical amino acid sequences in all 10 hypervariable region clones indicated a very low degree of diversity. The hypervariable region sequence of the JFH-1 strain also exhibited monoclonality,[10] which can be important for efficient replication in cultured cells.

Subgenomic replicons SGR-S310/A and SGR-S310/B were constructed and their replication efficiency was evaluated by G418-resistant colony-formation assay. After 3 weeks, a small number of colonies were visible for both replicons (Figure 1*A*). Because more colonies were observed in SGR-S310/A than in SGR-S310/B, we focused on SGR-S310/A (henceforth called SGR-S310). Ten cell colonies of SGR-S310 were isolated and analyzed for HCV replication. The mean RNA titer was $9.1 \times 10^7 \pm 4.6 \times 10^7$ copies/μg total RNA (Figure 1*B*). HCV RNA (approximately 8 kb) was detected by Northern blotting (Supplementary Figure 2*A*). Viral proteins in the replicon cells were detected by immunofluorescence and Western blotting (Supplementary Figure 2*B* and 2*C*). To determine whether the G418 resistance of the cells was transmissible by cellular RNA transfection, we electroporated total cellular RNA isolated from 4 replicon clones into naïve HuH-7 cells. Multiple G418-resistant colonies appeared after transfection of the RNA isolated from the replicon clones (Supplementary Figure 3*A*), but not from the naïve HuH-7 cells. These results indicate that the replicon RNA in the parental colonies could replicate in naïve cells. Thus, the G418-resistant colonies that were isolated from cells electroporated with SGR-S310 synthetic RNA contained replicating viral RNA.

Replicating genomes have been shown to accumulate cell culture adaptive mutations, which increase their replication potential. To examine whether SGR-S310 acquired mutations, the complete HCV sequences from 10 replicon clones were sequenced. At least one nonsynonymous mutation was detected in the NS3-NS5B region of each replicon clone (Figure 1B). The following mutations were identified: T1286I in the NS3 helicase (6 of 10

Abbreviation used in this paper: HCV, hepatitis C virus.

0016-5085/$36.00
http://dx.doi.org/10.1053/j.gastro.2012.09.017

A

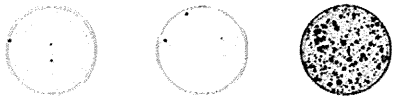

SGR-S310/A 10 μg | SGR-S310/B 10 μg | SGR-JFH1 0.1 μg

B

Replicon cell clone	Nucleotide mutation	Amino acid substitution	Affected protein	Replicon RNA amounts (copies/μg RNA)
1	5272 (6932) G→A	2198 R→H	NS5A	2.1×10^8
2	7362 (9022) A→G	2895 R→G	NS5B	9.9×10^7
3	2536 (4196) C→T	1286 T→I	NS3	9.5×10^7
4	2536 (4196) C→T	1286 T→I	NS3	9.9×10^7
5	2536 (4196) C→T	1286 T→I	NS3	5.6×10^7
6	2536 (4196) C→T	1286 T→I	NS3	4.0×10^7
7	2536 (4196) C→T	1286 T→I	NS3	8.3×10^7
8	2536 (4196) C→T	1286 T→I	NS3	8.7×10^7
9	6166 (7826) C→T	2496 T→I	NS5B	9.3×10^7
	7363 (9023) G→A	2895 R→K	NS5B	
10	5241 (6901) A→G	2188 T→A	NS5A	5.1×10^7

C

Replicon constructs	Protein	Colony formation efficiency (cfu/μg RNA)	Transient replication efficiency (72h/4h†)
SGR-S310/A	None	0.4×10^0	4.4×10^{-3}
T1286I	NS3	2.9×10^3	6.5×10^{-3}
T2188A	NS5A	2.3×10^2	4.9×10^{-3}
R2198H	NS5A	3.7×10^3	6.0×10^{-2}
S2210I	NS5A	6.2×10^2	1.1×10^{-2}
T2496I	NS5B	0.2×10^0	5.0×10^{-3}
R2895K	NS5B	2.3×10^3	7.9×10^{-2}
R2895G	NS5B	9.8×10^2	2.6×10^{-2}
T2496I+R2895K	NS5B	4.1×10^3	2.6×10^{-1}
Con1-NK5.1	NS3+NS5A	9.1×10^2	6.3×10^0
N	None	NA††	7.1×10^{-2}
SGR-JFH1	None	5.3×10^3	1.5×10^2

Figure 1. S310 subgenomic replicon analysis. (*A*) Three million HuH-7 cells were electroporated with 10 μg RNA from SGR-S310/A or SGR-S310/B or 0.1 μg RNA from SGR-JFH1. G418-selected colonies were fixed and stained after 3 weeks. (*B*) Non-synonymous mutations identified in the replicon genomes and HCV RNA titers in the replicon clones. Nucleotide positions within the S310 subgenomic replicon and within the full-length S310 genome (in parentheses) are given. (*C*) Replication potential of the adaptive mutants as determined by the colony-formation assay using Neo-replicons and by the transient replication assay using Fluc-replicons. †72 h/4 h, transient replication efficiency was determined as a ratio of luciferase activity in the transfected cells between 72 h and 4 h post transfection. ††NA, not available.

clones); T2188A or R2198H in NS5A (2 clones); an R2895G substitution in NS5B (1 clone); and T2496I in NS5A plus R2895K in NS5B (1 clone). These mutations and the S2210I mutation (corresponding to S2204I in genotype 1 replicon)[7,8] were introduced, individually or in combination, into the parental SGR-S310 and the colony-formation efficiencies of the mutant replicons were tested. All mutations, except T2496I, increased the colony formation, indicating an adaptive phenotype (Figure 1*C*, Supplementary Figure 3*B*). Transient replication efficiency was also tested using firefly luciferase reporter replicons. SGR-S310/Luc did not replicate in Huh-7.5.1 cells, whereas the adaptive mutants displayed varying degrees of replication (Figure 1*C*, Supplementary Figure 3*C*). Adaptive mutations T2496I and R2895K, when combined together, most efficiently enhanced the colony formation as well as transient replication (Figure 1*C*). Interestingly, T1286I and R2895G found in our study correspond to the Con1 adaptive mutations T1280I and R2884G, respectively.[11,12] T2188A or R2198H in NS5A were identified in 2 replicon clones and are located close to S2210I. Indeed, S2210I also enhanced SGR-S310 replication, suggesting that this region might be important for HCV replication. S310 replicons with adaptive mutations were compared with genotype 1b (Con1 and N) and 2a (JFH-1) replicons. Colony-formation efficiencies of most S310 adaptive replicons were at levels comparable with Con1 and JFH-1 (Figure 1*C*, Supplementary Figure 3*B*). In contrast, S310 adaptive replicons replicated less efficiently than Con1-NK5.1 and JFH-1 replicons in transient replication assays. However, genotype 1b N replicon replicated at a level similar to some S310 adaptive replicons (Figure 1*C*, Supplementary Figure 3*C*). Future studies will dissect the detailed mechanisms that underlie the effects of these mutations.

Successful generation of a genotype 3a replicon provided a unique opportunity to compare the susceptibility of genotype 3a (SGR-S310), 1b (Con1[13]), and 2a (JFH-1/4-1[13]) replicons to HCV inhibitors. Interferon-alfa dose-dependently decreased the replication of all tested genotypes (Figure 2*A*), whereas a protease inhibitor, BILN-2061, was more effective against replicons from genotypes 1b and 2a than 3a (Figure 2*B*). The non-nucleoside polymerase inhibitor JTK-109 was more potent against genotype 1b and 3a (Figure 2*C*). However, the nucleoside polymerase inhibitor, PSI-6130, equally inhibited all genotypes (Figure 2*D*).

In conclusion, we established a subgenomic replicon for genotype 3a, which should be useful for understanding the specific characteristics of this genotype and for the screening of antiviral chemicals that are effective against this genotype. Construction of a full-length infectious S310 clone is in progress.

Supplementary Material

Note: To access the supplementary material accompanying this article, visit the online version of *Gastroenterology* at www.gastrojournal.org, and at http://dx.doi.org/10.1053/j.gastro.2012.09.017.

References

1. Di Bisceglie AM. Hepatology 1997;26(Suppl):34S–38S.
2. Lauer GM, et al. N Engl J Med 2001;345:41–52.
3. Ohno T, et al. J Clin Microbiol 1997;35:201–207.
4. Hui JM, et al. J Gastroenterol Hepatol 2002;17:873–881.
5. Gottwein, JM et al. Gastroenterology 2011;141:1067–1079.
6. Lohmann, V et al. Science 1999;285:110–113.
7. Blight KJ, et al. Science 2000;290:1972–1974.
8. Blight KJ, et al. J Virol 2003;77:3181–3190.
9. Kato T, et al. Gastroenterology 2003;125:1808–1817.
10. Kato T, et al. J Med Virol 2001;64:334–339.
11. Krieger N, et al. J Virol 2001;75:4614–4624.
12. Lohmann V, et al. J Virol 2001;75:1437–1449.

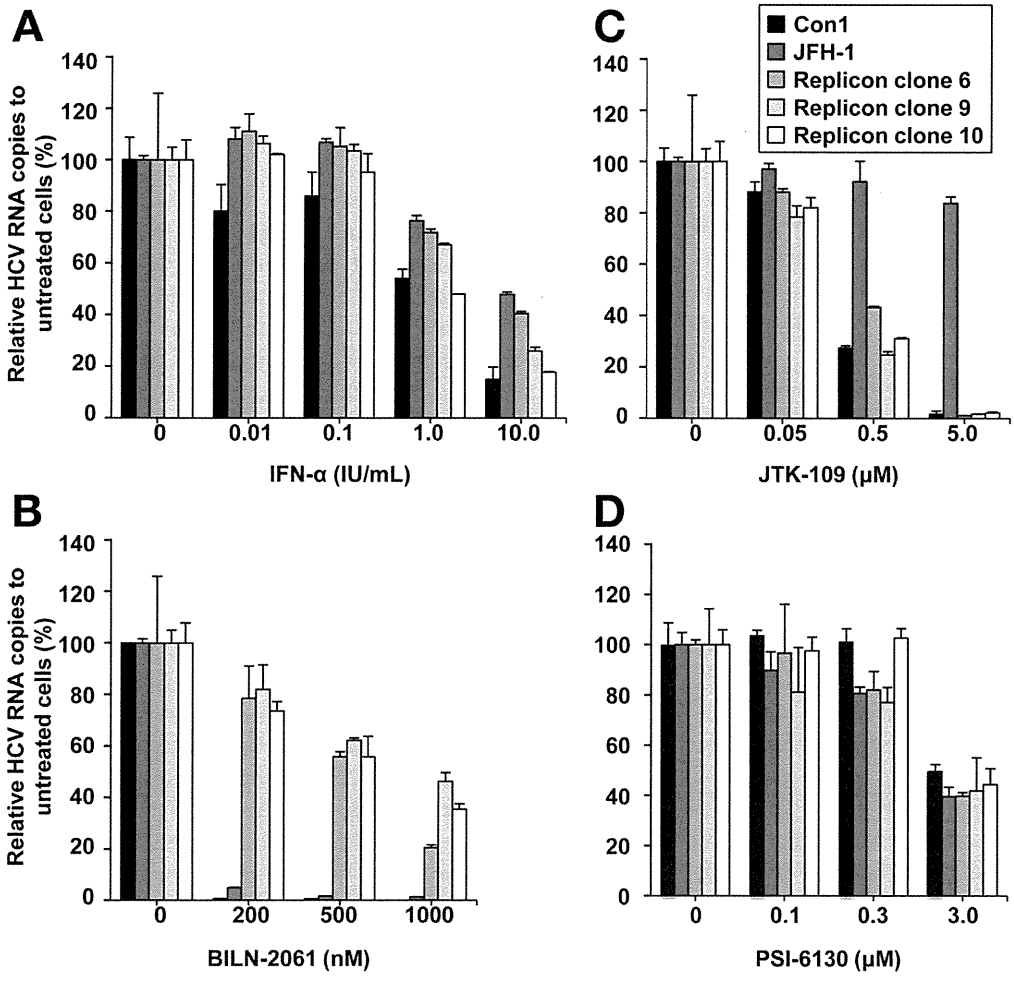

Figure 2. Effects of antiviral inhibitors on the replication of S310 subgenomic replicons. Three cell clones (clone 6, 9 and 10) carrying genotype 3a S310 replicons and one cell clone each harboring genotype 1b Con1 and genotype 2a JFH-1 replicons were treated with the indicated concentrations of (A) interferon alpha, (B) HCV protease inhibitor BILN-2061, (C) the non-nucleoside polymerase inhibitor JTK-109, and (D) the nucleoside polymerase inhibitor PSI 6130 for 72 hours and replication levels were measured by quantifying intracellular HCV RNA. Results are means ± standard deviations of 3 replicates.

13. Miyamoto M, et al. Intervirology 2006;49:37–43.

Received February 22, 2012. Accepted September 10, 2012.

Reprint requests

Address requests for reprints to: Takaji Wakita, MD, PhD, Department of Virology II, National Institute of Infectious Diseases, 1-23-1 Toyama, Shinjuku-ku, Tokyo 162-8640, Japan. e-mail: wakita@nih.go.jp; fax: +81-3-5285-1161.

Acknowledgments

Huh-7.5.1 cells were kindly provided by Dr Francis V. Chisari. BILN-2061, JTK-109, and PSI-6130 were generous gifts from Boehringer Ingelheim (Canada) Ltd., Japan Tobacco, Inc., and Pharmasset, Inc., respectively. Con1-NK5.1 and N replicon constructs were kindly provided by Dr Ralf Bartenschlager and Dr Stanley Lemon, respectively. We thank Dr Hideki Aizaki and Dr Hussein H. Aly for their helpful discussions. We also thank Ms Minako Kaga for her technical assistance.

DDBJ/EMBL/GenBank accession numbers: S310/A: AB691595, S310/B: AB691596, SGR-S310/A: AB691597, SGR-S310/B: AB691598, SGR-S310/Luc: AB691599.

Dr Saeed is presently at the Center for the Study of Hepatitis C, The Rockefeller University, New York, NY.

Dr Suzuki is presently at Department of Infectious Diseases, Hamamatsu University School of Medicine, Hamamatsu, Japan.

Conflicts of interest

The authors disclose no conflicts.

Funding

This work was partially supported by Grants-in-Aid for Scientific Research from the Japan Society for the Promotion of Science, from the Ministry of Health, Labour and Welfare of Japan, from the Ministry of Education, Culture, Sports, Science and Technology, from the National Institute of Biomedical Innovation, and by the Research on Health Sciences Focusing on Drug Innovation from the Japan Health Sciences Foundation and from the French Agence Nationale de la Recherche sur le SIDA et les Hépatites Virales (ANRS, contract 07306).

Supplementary Methods

Cell Culture

The human hepatoma cell line HuH-7[1] and its derivative cell line Huh-7.5.1[2] were maintained in Dulbecco's modified Eagle medium supplemented with 10% fetal bovine serum, minimal essential medium nonessential amino acids, 100 U/mL penicillin, 100 μg/mL streptomycin, 10 mM HEPES, and 1 mM sodium pyruvate at 37°C in a 5% CO_2 incubator.

Primary human hepatocytes (PHH) were isolated from an encapsulated liver sample.[3] Isolated PHH were seeded in 12-well plates and cultured at 37°C in Lanford medium before infection.

PHH Infection With HCV-Positive Sera

Three days post seeding, PHH were inoculated with HCV-positive sera. After 16 h of inoculation, monolayers were washed with William's E medium and fresh Lanford medium was added. Cells were harvested at 72 h post infection. Total RNA was isolated using a guanidinium isothiocyanate solution (RNAble; Eurobio, Courtaboeuf, France) and intracellular levels of HCV RNA were quantified using the SuperScript III Platinium One-Step quantitative reverse transcription polymerase chain reaction (RT-PCR) system (Invitrogen, Carlsbad, CA) and a LightCycler480 real-time PCR system (Roche Diagnostics, Meylan, France).

HCV Genotype 3a Clone

Clone S310 was isolated from a 71-year-old female patient suffering from post liver transplantation HCV recurrence. She was diagnosed with HCV genotype 3a infection at the age of 59 years and underwent liver transplantation 4 years later due to liver cirrhosis. HCV-RNA titer was 2.8×10^6 copies/mL. Total RNA extracted from 100 μL serum using the acid-guanidinium isothiocyanate-phenol-chloroform method (Isogen-LS; Nippon Gene, Tokyo, Japan) was precipitated with isopropanol, washed with ethanol, and dissolved in 10 μL nuclease-free water. An aliquot of 4 μL was subjected to reverse transcription using random hexamers and Moloney murine leukemia virus reverse transcriptase (Superscript III; Invitrogen) at 42°C for 50 min and then at 50°C for 10 min.

Isolation of HCV

The sequences of 4 isolates of genotype 3a (accession numbers AF046866, D28917,[4] X76918, and D17763[5]) that were obtained from the HCV database (http://hcv.lanl.gov/content/sequence/HCV/ToolsOutline.html) were aligned and PCR primers were designed based on the conserved sequences. These primers were used to amplify the complementary DNA (cDNA) of S310 into 9 overlapping fragments by nested PCR (nt 1–370, nt 127–1284, nt 1117–1997, nt 1704–3352, nt 3152–5080, nt 4869–6842, nt 6601–8129, nt 7988–9145, and nt 9082–9576; nucleotide numbers refer to the positions on S310, with nt 1 being the first nucleotide of the 5′ UTR). The sequence of these primers is shown in Supplementary Table 1. Two microliters of cDNA was subjected to PCR using Pyrobest DNA polymerase (Takara Bio, Kyoto, Japan) and the outer set of primers, and this first-round PCR product (2 μL) was further amplified by a second round of PCR using the inner set of primers. PCR conditions for the first and second rounds of PCR consisted of 35 cycles each of denaturation at 98°C for 20 s, annealing at 55°C for 1 min, and extension at 72°C for 3 min. A fragment encompassing the 5′ end of the viral genome (nt 1–370) was amplified by 5′RACE. Briefly, cDNA was synthesized with a 5′ UTR primer (antisense), tailed with a dCTP homopolymer by using terminal deoxynucleotidyl transferase, and amplified by PCR (5′ RACE System for Rapid Amplification of cDNA Ends; Invitrogen) using TaKaRa LA Taq polymerase (Takara Bio). The PCR products of all fragments were separated by agarose gel electrophoresis, cloned into the pGEM-T EASY vector (Promega, Madison, WI) and sequenced using the Big Dye Terminator Mix and an automated DNA sequencer. The consensus sequence of 5 to 9 isolated cDNA clones was adopted for each fragment. Two major populations of the virus were identified in the patient's serum that differed in 4 amino acids in the NS3 protein (aa 1039, 1183, 1463, and 1504), and these populations were designated as S310/A and S310/B (DDBJ/EMBL/GenBank accession number: AB691595 and AB691596, respectively). To assess the complexity of the HCV population in the patient's serum, the hypervariable region sequences of 10 clones were determined.

Computer Analysis

A phylogenetic tree was constructed using the neighbor-joining method to examine the relationship between the polyprotein region of S310 and that of other HCV genotype 3a isolates available in the database. In order to analyze the diversity in each subgenomic region, the genetic distance was calculated between all possible pairs of genotype 3a isolates and between S310/A and other isolates using MacVector software (MacVector, Inc., Cary, NC). The ratios of these 2 values (mean genetic distance between S310/A and other isolates/mean genetic distance among all genotype 3a isolates) were compared.

Construction of Replicons

Based on the consensus sequence of S310, we assembled pS310/A and pS310/B, which contained the full-length S310/A and S310/B cDNA, respectively, downstream of the T7 RNA polymerase promoter. Briefly the 9 amplicons described here were combined by overlapping PCR and ligated with pGEM-T EASY vectors to generate 6 plasmids (A through F) in such a way that each plasmid contained a unique restriction enzyme

cleavage site toward the 3′ end of the viral fragment, which overlapped with the 5′ end of the next fragment. For this purpose, we took advantage of the EcoRI restriction site that is present in the polycloning site of the plasmid toward the 5′ end of the viral fragment. Plasmid A contained the T7 promoter sequence followed by one G-nucleotide and nt 1–3352 of S310, while plasmids B, C, D, and E contained nt 1704–4307, nt 4044-6013, nt 5424–7755, and nt 7276–9425, respectively. Plasmid F contained the fragment constructed by combining the C-terminal end of NS5B (nt 9182–9402) and the variable and poly U/UC regions of the S310/A 3′UTR (nt 9403–9610) with the last 44 nucleotides of JFH-1. Restriction sites for EcoRI and XbaI were introduced upstream of the T7 promoter sequence and downstream of the conserved region, termed the *X-region*, of the 3′UTR, respectively, and the restriction sites of these enzymes that were present within the cDNA were removed by PCR-based mutagenesis. In the neomycin-based subgenomic replicons (SGR-S310/A and SGR-S310/B, accession number: AB691597 and AB691598, respectively), the cassette containing the neomycin phosphotransferase gene and the EMCV IRES replaced the region of S310 that encompasses amino acids 20–1032. Firefly luciferase–based subgenomic replicons (SGR-S310/Luc, accession number: AB691599) were generated from SGR-S310/A by replacing amino acids 20–1032 of S310/A with the cassette containing firefly luciferase and the EMCV IRES from pSGR-JFH1/Luc.[6]

RNA Synthesis

RNA was synthesized by in vitro transcription as described previously.[7] Briefly, the plasmids carrying the cDNA described here were linearized with the XbaI restriction enzyme and 5′ overhangs were removed by treating with mung bean nuclease. Reaction mixtures were further incubated at 50°C for 1 h with 2 μL 20 mg/mL proteinase K and 10 μL 10% sodium dodecyl sulfate to degrade nucleases, and templates were purified with 2 rounds of phenol-chloroform extraction and ethanol precipitation. Three micrograms of templates were subjected to in vitro transcription using a MEGAscript T7 kit (Ambion, Austin, TX) according to the manufacturer's recommendations. Synthesized RNA was treated with DNase I (Ambion) and then purified using ISOGEN-LS (Nippon Gene). The quality of the synthesized RNA was examined by agarose gel electrophoresis.

RNA Transfection

In vitro transcribed RNA or total cellular RNA isolated from replicon cells was introduced into cells by electroporation. Trypsinized cells were washed twice with serum-free Opti-MEM I (Invitrogen) and 3.0×10^6 cells were resuspended in 400 μL cytomix buffer.[8] RNA was delivered into cells by a single pulse of 260 V and 950 μF using the Bio-Rad Gene Pulser II apparatus (Bio-Rad, Hercules, CA). Transfected cells were immediately suspended in culture medium and transferred to the appropriate plates. For G418 selection of colonies, the transfected cells were seeded in 10-cm dishes, each containing 8 mL culture medium. G418 (500 μg/mL; Nacalai Tesque, Kyoto, Japan) was added to the culture medium at 24 h after transfection. Culture medium supplemented with G418 was replaced every 3 days. Three weeks after transfection, cells were fixed with buffered formalin and stained with crystal violet or replicon colonies were picked and expanded.

Analysis of G418-Resistant Cells

G418-resistant colonies were collected and used for further analysis. Colonies were independently isolated using cloning cylinders (Asahi Techno Glass Co., Tokyo, Japan) and were expanded until they were 80%–90% confluent in 10-cm dishes. Expanded cells were harvested for nucleic acid and protein analysis. Total RNA was isolated from the cells using the ISOGEN reagent (Nippon Gene). Another aliquot of the cell pellet was dissolved in RIPA buffer containing 0.1% sodium dodecyl sulfate for Western blot analysis. For immunofluorescence analysis of viral proteins, cells were seeded on 12-well slides.

Quantification of HCV RNA by Real-Time RT-PCR

Copy numbers of HCV RNA were determined by real-time detection RT-PCR, as described previously,[9] using the ABI Prism 7700 Sequence Detector System (Applied Biosystems Japan, Tokyo, Japan). The concentration of total RNA in the cells was determined using a Nanodrop Spectrophotometer ND-1000 (Thermo Scientific, Rockford, IL).

Northern Blot Analysis

Isolated RNAs (3 μg) from replicon cells were separated on a 1% agarose gel containing formaldehyde, transferred to a positively charged nylon membrane (Hybond-N+; GE Healthcare UK Ltd., Buckinghamshire, UK) and immobilized using a FUNA-UV-LINKER (Funakoshi, Tokyo, Japan). Hybridization was carried out with a [α-^{32}P]dCTP-labeled DNA probe using Rapid-Hyb buffer (GE Healthcare UK Ltd.). The DNA probe was synthesized from a BsrGI-MfeI fragment of the S310 clone that contained NS3-5B genes using the Megaprime DNA labeling system (GE Healthcare UK Ltd.).

Indirect Immunofluorescence

Untransfected HuH-7 cells or S310 replicon-replicating cells were grown on a glass slide for 24 h and fixed in acetone-methanol (1:1 [vol/vol]) for 10 min at −20°C. Cells were then incubated in immunofluorescence buffer (phosphate-buffered saline, 1% bovine serum albumin, 2.5 mM EDTA). S310 patient serum was added at

a dilution of 1:200 in immunofluorescence buffer. After incubation for 1 h at room temperature, cells were washed and then incubated with an Alexa Fluor488–conjugated goat anti-human IgG antibody (Invitrogen) in immunofluorescence buffer. The glass slide was washed and a cover glass was mounted using PermaFluor mounting solution (Thermo Scientific, Cheshire, UK). Cells were examined under a fluorescence microscope (Olympus, Tokyo, Japan).

Western Blot Analysis of HCV Proteins

The protein samples were separated on 12.5% polyacrylamide gels and subsequently transferred to a polyvinylidene difluoride membrane (Immobilon; Millipore, Bedford, MA). Transferred proteins were incubated with 2% skim milk. Anti-NS3 mouse monoclonal antibody (clone 8G2, Abcam, Cambridge, UK) and peroxidase-labeled sheep anti-mouse IgG (Cell Signaling Technology, Danvers, MA) were used to detect HCV proteins. The signals were detected with a chemiluminescence system (ECL Prime; GE Healthcare UK Ltd.).

Identification of Mutations

cDNA was synthesized from total RNA that was extracted from replicon-expressing cells at 2 different times. These cDNAs were amplified into 5 overlapping fragments that spanned the 5′UTR and the NS3-NS5B region using LA Taq DNA polymerase (Takara Bio) and the primers described in Supplementary Table 1. The sequence of each amplified DNA was determined. The mutations identified were subsequently introduced into SGR-S310/A and SGR-S310/Luc by PCR-mediated mutagenesis.

Luciferase Assay

Five micrograms of RNA, prepared by in vitro transcription of S310/SG-FLuc constructs with or without adaptive mutations, were introduced into 3.0×10^6 Huh-7.5.1 cells by electroporation. Cells were harvested with Cell Culture Lysis Reagent (Promega) at 4, 24, 72, and 96 h post electroporation, and luciferase activity was determined by use of a Luciferase Assay System (Promega) and the Lumat LB9507 luminometer (EG & G Berthold, Bad Wildbad, Germany).

Inhibition of S310 Replicon Replication by Specific Inhibitors

S310 replicon cell clones 6, 9, and 10 and the genotype1b Con1 and 2a JFH-1 replicon cells,[10] were seeded into 24-well plates at a density of 5.0×10^4 cells/well. On the next day, the culture medium was replaced with medium containing 0.1% dimethyl sulfoxide with or without various concentrations of interferon alfa (Dainippon-Sumitomo, Osaka, Japan), the specific NS3 protease inhibitor, BILN-2061 (Boehringer Ingelheim Ltd., Québec, Canada), or the NS5B inhibitors, JTK-109 (Japan Tobacco, Inc., Osaka, Japan) and PSI-6130 (Pharmasset, Inc., Princeton, NJ). After 72-h incubation, cells were harvested and HCV RNA was quantified as described.

Supplementary References

1. Nakabayashi H, et al. Cancer Res 1982;42:3858–3863.
2. Zhong J, et al. Proc Natl Acad Sci U S A 2005;102:9294–9299.
3. Pichard L, et al. Methods Mol Biol 2006;320:283–293.
4. Yamada N, et al. J Gen Virol 1994;75:3279–3284.
5. Sakamoto M, et al. J Gen Virol 1994;75:1761–1768.
6. Kato T, et al. J Clin Microbiol 2005;43:5679–5684.
7. Wakita T, et al. Nat Med 2005;11:791–796.
8. van den Hoff MJ, et al. Nucleic Acids Res 1992;20:2902.
9. Takeuchi T, et al. Gastroenterology 1999;116:636–642.
10. Miyamoto M, et al. Intervirology 2006;49:37–43.